Nanoscale Horizons

ROYAL SOCIETY OF CHEMISTRY

REVIEW

View Article Online
View Journal | View Issue

Cite this: *Nanoscale Horiz.*, 2025, **10**, 3184

DNA nanotechnology-enabled bioanalysis of extracellular vesicles

Li Pan and Pengfei Wang *

Extracellular vesicles (EVs) have emerged as valuable sources for liquid biopsy in disease diagnostics, given their protein and nucleic acid cargoes (*e.g.*, miRNA, mRNA, glycoRNA) can serve as critical biomarkers. DNA nanotechnology, leveraging its inherent programmability, high specificity, and powerful signal amplification capability, offers a transformative approach for the bioanalysis of EVs. This review summarizes recent advances in DNA nanotechnology-based analytical methodologies for detecting EV-associated proteins and nucleic acids. We detail the underlying principles, applications, and performance of key strategies, including aptamer-based recognition, enzyme-free catalytic amplification circuits (*e.g.*, HCR, CHA), enzyme catalytic amplification techniques (*e.g.*, RCA, CRISPR-Cas systems), and DNA nanostructures-assisted amplification. The integration of these DNA tools into multiplexed detection platforms is also discussed. Finally, current challenges and future perspectives concerning clinical translation of EV detection are presented.

Received 4th August 2025,
Accepted 4th September 2025

DOI: 10.1039/d5nh00557d

rsc.li/nanoscale-horizons

1. Introduction

EVs represent promising circulating biomarkers for diagnosing and prognosing numerous diseases. Initially regarded as mere "platelet dust" serving to eliminate cellular debris,[1] EVs are now recognized as heterogeneous, membrane-bound vesicles secreted by cells *via* diverse biogenesis pathways.[2–4] Produced by virtually all cell types,[5,6] particularly by rapidly proliferating cancer cells,[7,8] EVs are abundant in bodily fluids (*e.g.*, blood, urine), constituting a stable and accessible source of circulating biomarkers.[9]

EVs encapsulate a diverse molecular repertoire,[10–12] including proteins, nucleic acids, lipids, metabolic molecules and so on. These cargoes exist in distinct organizational states: either as intrinsic EV constituents inherited directly from parent cells, or as membrane-associated entities. This association may reflect unique biophysical and biochemical properties of both the vesicles and bound molecules. Through their molecular contents, EVs function as critical mediators of intercellular communication. By shuttling biological molecules between cells, EVs modulate local and distant microenvironments,[13] thereby propagating diverse pathophysiological processes.

Due to the low abundance of EVs in biofluids, and the complexity of the sample matrix pose significant challenges for detection. DNA molecules, governed by precise Watson–Crick base pairing, offer unique advantages: ease of chemical modification, designability into diverse functional structures,[14–16] and powerful isothermal amplification capabilities. These properties make DNA

Institute of Molecular Medicine, Shanghai Key Laboratory for Nucleic Acid Chemistry and Nanomedicine, Renji Hospital, School of Medicine, Shanghai Jiao Tong University, Shanghai, 200127, China. E-mail: pengfei.wang@sjtu.edu.cn

Li Pan

Li Pan received her PhD degree in 2019 from Jackson State University, USA. She currently works as an assistant professor at the Institute of Molecular Medicine, School of Medicine, Shanghai Jiao Tong University, China. She currently focuses on the development of new biosensing methods.

Pengfei Wang

Pengfei Wang is a professor at the Institute of Molecular Medicine, School of Medicine, Shanghai Jiao Tong University, China. He earned his PhD degree in biomedical engineering from Purdue University, USA, in 2014. His current research interests include nucleic acid bionanotechnology, biosensing, liquid biopsy etc.

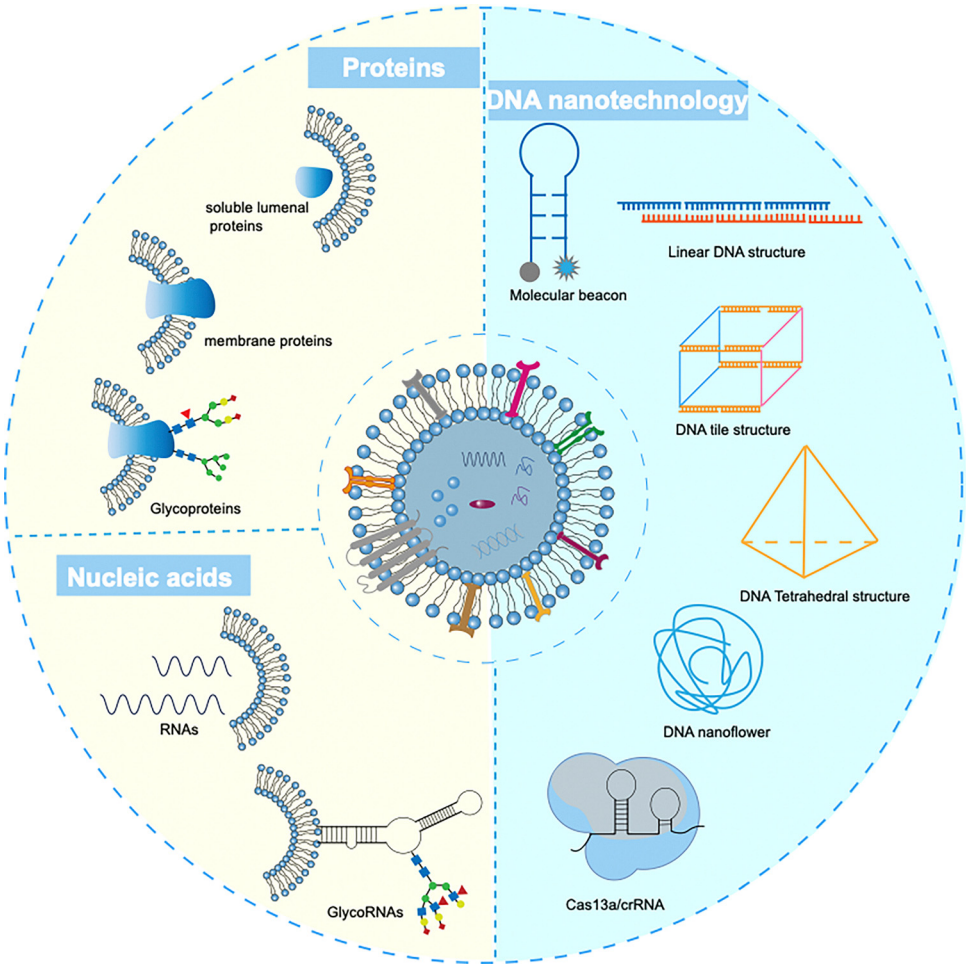

Fig. 1 Schematic illustration of DNA nanotechnology for the detection of proteins and nucleic acids in EVs.

nanotechnology an exceptionally powerful toolkit for developing highly sensitive, specific, and multiplexed EV detection platforms. This review systematically explores the research strategies and advancements in DNA nanotechnology-driven detection of both EV proteins and nucleic acids (Fig. 1).

2. EVs as potential biomarkers

2.1. Biogenesis of EVs

EVs are primarily categorized based on their mechanism of biogenesis into three distinct subtypes: exosomes, microvesicles (ectosomes), and apoptotic bodies (Fig. 2A).[3,9,13] Exosomes are generated through the endosomal pathway, involving the inward budding of the endosomal membrane to form intraluminal vesicles (ILVs) within multivesicular bodies (MVBs). Mature MVBs subsequently undergo calcium-dependent fusion with the plasma membrane to release ILVs as exosomes into the extracellular space. Microvesicles (often termed ectosomes) form directly through outward budding and fission of the plasma membrane, a process driven by cytoskeletal rearrangements and calcium influx. Apoptotic bodies are produced during the late stages of programmed cell death (apoptosis) as the cell undergoes fragmentation. Critically, due to overlapping physical properties (*e.g.*, size, density) upon secretion, conventional isolation methodologies cannot fully resolve these biogenetically distinct EV subpopulations.[10] Consequently, the term "exosomes" is frequently used operationally in the literature to denote heterogeneous isolates of small, sedimentable vesicles, often irrespective of precise biogenetic origin. In accordance with the minimal information for studies of extracellular vesicles (MISEV) guidelines established by the International Society for extracellular vesicles (ISEV),[17] this review utilizes the operational term "EVs" to encompass all secreted vesicle subtypes discussed, acknowledging the current technical limitations in definitive isolation. By operational definition, EVs with diameters below 200 nm are classified as small EVs (sEVs), while those exceeding 200 nm are designated large EVs (lEVs) (Fig. 2).

2.2. EV proteins

EVs hold significant promise as disease biomarkers due to their capacity to encapsulate and transport unique protein signatures reflective of specific patient pathophysiological states. These EV-associated bioactive molecules can modulate

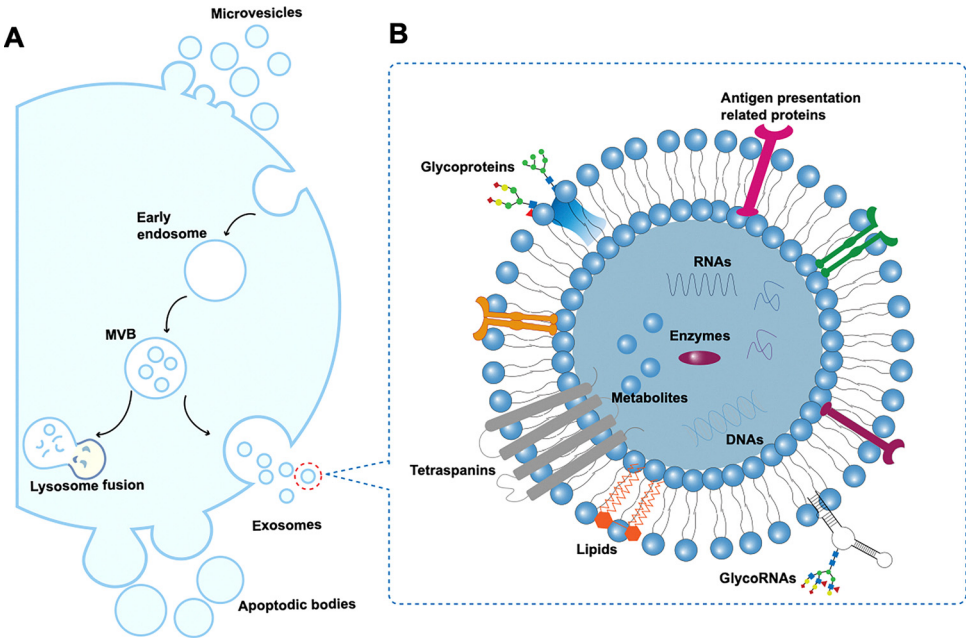

Fig. 2 Intracellular pathways of EV biogenesis (A) and their contents (B).

recipient cell behavior and represent valuable targets for both therapeutic and diagnostic applications.[18] While proteins present on EVs generally retain their core biochemical functions, their biological roles diverge significantly from those observed on the cell surface. On the plasma membrane, such proteins primarily mediate direct signaling and cell–cell interactions.[19] In contrast, when incorporated into EVs, they become instrumental in critical processes including cargo sorting during EV biogenesis, directing EV targeting to specific recipient cells, facilitating EV uptake, and enabling long-distance intercellular communication. Furthermore, the EV lumen and membrane confer a protective microenvironment, shielding these proteins from degradation. This preservation enhances the functional integrity of EV-associated proteins and significantly bolsters their utility as stable and reliable diagnostic biomarkers (Fig. 2A).[12,20]

2.2.1. Conventional protein markers. Canonical markers include the tetraspanin superfamily (*e.g.*, CD9, CD63, CD81),[20–23] components of the Endosomal Sorting Complex Required for Transport (ESCRT) machinery (*e.g.*, TSG101, ALIX),[24,25] heat shock proteins (Hsp70, Hsp90),[26,27] and membrane trafficking proteins (Rab GTPases, annexins).[28,29] These proteins constitute the structural framework of EVs, participating in vesicle biogenesis, cargo sorting, and cellular targeting. Their expression profiles serve as key identifiers for EV subtyping. Tetraspanins organize membrane microdomains to regulate signal transduction, ESCRT complexes mediate the intraluminal sorting of ubiquitinated proteins, and heat shock proteins maintain the folding stability and functional integrity of luminal cargo.

2.2.2. Cancer-associated protein biomarkers. Beyond conventional markers essential for EV function, EVs encapsulate biomolecules specifically expressed or enriched within their parent cells, enabling identification of cellular origin. Cancer-associated protein biomarkers exhibit pathognomonic expression within EVs. The transmembrane receptor CD44, binding hyaluronic acid, promotes metastatic dissemination, and $CD44^+$ EVs serve as markers for tracking cancer stem cells.[30,31] The immune checkpoint protein CD47 facilitates immune evasion through interaction with SIRPα on phagocytes, with $CD47^+$ EV levels correlating positively with tumor progression.[32] Glycoproteins defined by covalently attached glycans, are integral components of EVs. They play pivotal roles in EV biogenesis, cargo sorting, intercellular communication, and recipient cell targeting. Glycoproteins hold significant diagnostic value in oncology: epithelial cell adhesion molecule (EpCAM), an *N*-linked glycoprotein, is enriched in EVs derived from epithelial carcinomas;[33,34] glypican-1 (GPC1), another *N*-linked glycoprotein, is a prominent biomarker for early pancreatic cancer detection;[35] and Mucin-1 (MUC1), a heavily *O*-glycosylated protein, shows specific enrichment in breast cancer EVs.[36,37] The glycosylation patterns of these glycoproteins critically influence EV stability, cellular uptake efficiency, and immunomodulatory properties,[38,39] forming a molecular basis for disease stratification (Fig. 2B).

2.3. EV nucleic acids

EVs encapsulate a diverse repertoire of RNA species, reflecting the genetic and functional heterogeneity of their parent cells. This includes small RNAs (microRNAs), small interfering RNAs (siRNAs), small nuclear RNAs (snRNAs), small nucleolar RNAs (snoRNAs), PIWI-interacting RNAs (piRNAs, Y RNAs, ribosomal RNAs (rRNAs), long non-coding RNAs (lncRNAs), circular RNAs (circRNAs), messenger RNAs (mRNAs), precursor RNAs, transfer RNAs (tRNAs), and mitochondrial RNAs (mtRNAs).[40,41] These EV-associated RNAs orchestrate critical biological processes including gene regulation, cellular signaling, and disease pathogenesis, establishing their utility as valuable biomarkers for early diagnosis and therapeutic targeting.[42] Specific RNA classes demonstrate

distinct biomarker potential. miRNAs regulate post-transcriptional gene expression and are implicated in cancer, cardiovascular diseases, and neurodegenerative disorders.[43] siRNAs offer therapeutic promise *via* RNA interference for targeting genes in viral infections and genetic diseases.[44] circRNAs function as miRNA sponges, influencing cancer progression and neurodegeneration.[45] lncRNAs modulate chromatin dynamics and gene expression, contributing to cancer biology and cardiovascular disorders.[46]

mRNA profiles within EVs mirror the gene expression status of originating cells, providing insights into disease progression and treatment response.[47,48] tRNAs and mtRNAs serve as indicators of cellular metabolism and mitochondrial dysfunction, relevant to cancer and neurodegeneration.[49] Short non-coding RNAs (snRNAs, snoRNAs, Y RNAs, piRNAs, rRNAs) are essential for RNA processing, protein synthesis, and cellular homeostasis, with significant biomarker implications for genetic disorders and cancer.[50] The RNA composition of EVs is distinct from their parental cells, exhibiting enrichment in small RNAs (*e.g.*, miRNAs) and fragmentation or truncation of longer RNAs (*e.g.*, mRNAs). In contrast, parental cells predominantly contain intact, full-length mRNAs. Mammalian cell total RNA spans ~20–12 000 nucleotides (nt), predominantly comprising rRNA (80–90% total RNA, including 18S/28S subunits). While truncated rRNA subunits are frequently detected in EVs, full-length mRNAs are less common and primarily associated with larger EV subtypes (lEVs), constrained by the limited nucleic acid capacity (typically ~10 000 nt) of small EVs (sEVs).[51–54] EVs also harbor diverse DNA species, including double-stranded DNA (dsDNA), single-stranded DNA (ssDNA), mitochondrial DNA (mtDNA), viral DNA, and genomic DNA (gDNA).[55] Each type contributes uniquely to intercellular communication and disease pathogenesis. dsDNA facilitates intercellular genetic exchange and disease propagation, ssDNA supports viral infection and genetic maintenance, mtDNA signals cellular stress and modulates immunity, viral DNA promotes infection spread and immune evasion, and gDNA influences recipient cell behavior.[56] Surface glycosylation of nucleic acids represents a non-canonical post-transcriptional modification recently identified on EVs. While nucleic acids (*e.g.*, RNA/DNA) are conventionally encapsulated within the EV lumen or membrane-bound compartments, emerging evidence indicates that specific nucleic acid species may undergo covalent glycosylation and localize to the EV surface. These glycosylated nucleic acids, predominantly observed as small non-coding RNAs (*e.g.*, miRNAs, Y RNAs) covalently linked to *N*-acetylgalactosamine (GalNAc) or sialylated glycans, defy traditional paradigms of nucleic acid compartmentalization.

3. Traditional detection methods for EV proteins and nuclei acids

Western blotting (WB) remains the predominant technique for EV protein analysis.[57] This approach requires initial exosome isolation, followed by electrophoretic protein separation and immunodetection of EV-specific markers (*e.g.*, CD63, CD81) using target-specific antibodies. However, WB exhibits critical limitations: semi-quantitative output, extended processing time, substantial sample requirements, and limited suitability for clinical diagnostics. Enzyme-linked immunosorbent assay (ELISA) provides an alternative protein quantification platform through antibody–antigen binding coupled with enzymatic chromogenic reactions.[58] While less technically demanding and more quantitative than WB, conventional ELISA kits suffer from insufficient sensitivity for low-abundance EV targets. Flow cytometry methodologies, including bead-conjugated assays (*e.g.*, magnetic/silica beads) and emerging nanoscale flow cytometry, enable rapid surface protein profiling of individual EVs.[59] These techniques permit high-throughput enumeration of EV surface markers but remain constrained by specialized instrumentation requirements.

For EV nucleic acid quantification, reverse transcription polymerase chain reaction (RT-PCR) is considered the reference standard.[60] It employs sequence-specific primers to amplify targets, with fluorescence-based quantification achieving high sensitivity for low-copy nucleic acid. Nevertheless, RT-PCR necessitates prior nucleic acid extraction from lysed EV, requires large sample volumes, and demonstrates inter-assay variability that limits utility in large-scale cancer screening. Microarray technology facilitates multiplexed nucleic acid detection *via* reverse-transcribed DNA hybridization to array-immobilized probes.[61] While enabling high-throughput analysis, this method is prone to cross-hybridization artifacts and false-positive signals. Next-generation sequencing (NGS) offers superior specificity and comprehensive nucleic acid profiling but incurs elevated equipment costs and prolonged turnaround times. Critically, most current nucleic acid detection platforms require EV lysis, a process that risks nucleic acid degradation and introduces analytical bias.

4. DNA nanotechnology-enabled EV protein detection

EV proteins are key identifiers of cellular origin and tissue specificity (*e.g.*, CD9, CD63, CD81, EpCAM, PSMA). DNA-based technologies primarily utilize high-affinity ligands (mainly aptamers) coupled with efficient signal amplification strategies for protein detection.

4.1. Amplification-free detection of EV proteins using DNA aptamers

Aptamers are single-stranded DNA or RNA molecules selected *via* Systematic Evolution of Ligands by EXponential enrichment (SELEX) to bind specific target proteins with high affinity and specificity.[62,63] Compared to antibodies, aptamers offer smaller size, ease of synthesis and modification, superior stability, minimal batch-to-batch variation, and the ability to target non-immunogenic molecules. Aptamers serve as versatile recognition elements in EV detection platforms, typically implemented through two primary configurations: (i) immobilized on sensor surfaces (*e.g.*, functionalized gold electrodes,

quartz crystal microbalances, plasmonic nanoparticles) to capture target protein-bearing EVs, or (ii) deployed in solution phase for direct interaction with EVs. Subsequent target-specific binding events are transduced into measurable signals through either labeled reporters (fluorophores, enzymes, metallic nanoparticles) or structure-switching conformational changes in the aptamers themselves.

Optical platforms leverage light-matter interactions for sensitive detection, exemplified by FRET-based systems where aptamer-conjugated quantum dots transfer energy to AIEgen dyes upon EV membrane protein binding, achieving isolation-free lung cancer diagnosis with 100% accuracy/sensitivity in clinical cohorts using only 1 μL samples and machine learning-enhanced multi-biomarker profiling (Fig. 3A).[64] Similarly, homogeneous fluorescence polarization assays utilize antibody capture with secondary aptamer detection for dual-target specificity, reaching 5×10^6 EVs per mL sensitivity while eliminating purification steps and enabling real-time therapeutic monitoring through clinical analyzer compatibility.[65] Moreover, an aptamer-nanoflow cytometry (nFCM) integration enabling rapid multiplexed sEV protein profiling. Seven cancer-associated biomarkers (CA125, STIP1, CD24, EpCAM, EGFR, MUC1, HER2) were simultaneously labeled *via* aptamer probes and quantified in plasma-derived sEVs within minutes (Fig. 3B).[66] Electrochemical platforms transform binding events into electrical signals through innovative transduction mechanisms. The conformational switch strategy exploits methylene blue (MB) intercalation with guanine bases in anti-EpCAM aptamers (SYL3C), where target exosome binding induces structural changes that reduce MB electron transfer, creating an amplification-free "electronic switch" with ultrahigh sensitivity (234 particles per mL) for NSCLC diagnosis (Fig. 3C).[67] For multiplexed analysis, sequential labeling platforms combine aptamer-conjugated nanotags with bleomycin-Fe^{2+} cleavage cascades, enabling steric interference-free quantification of EGFR/PD-L1 co-expression at single-EV resolution (341 particles per mL) for TNBC patient stratification.[68] Further enhancing simplicity, ratiometric systems utilize DSPE-PEG phospholipids as dual-function agents: capturing EVs while serving as intrinsic redox probes whose diminished activity upon membrane insertion is measured against MB-labeled aptamer signals, achieving 811 particles per mL detection of CD63/HER2 in breast cancer plasma without signal amplification.[69] Microfluidic platforms enable complex

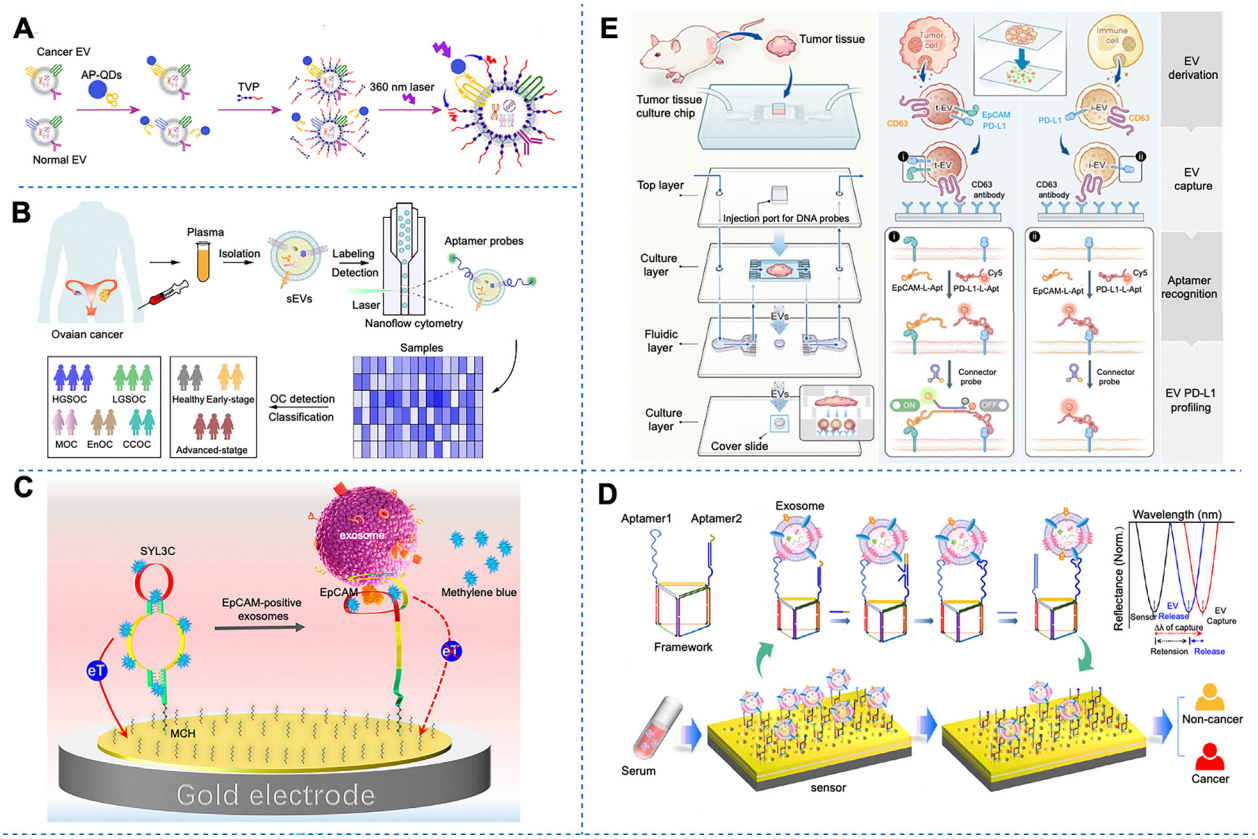

Fig. 3 Amplification-free detection of EV proteins using DNA aptamers. (A) Detection of EV membrane proteins *via* Förster resonance energy transfer. Reproduced with permission.[64] Copyright: 2023, American Chemical Society. (B) An aptamer-based nanoflow cytometry method for the molecular detection and classification of ovarian cancers. Reproduced with permission.[66] Copyright: 2023, John Wiley and Sons. (C) Single-stranded DNA aptamers as a highly efficient electronic switch for EV detection. Reproduced with permission.[67] Copyright: 2023, American Chemical Society. (D) A retention-monitoring assay based on logic profiling nucleic acid framework for accurate identification of EVs. Reproduced with permission.[73] Copyright: 2025, American Chemical Society. (E) Dual-switch aptamer logic gates-based microfluidic replication and phenotypic profiling of EV. Reproduced with permission.[70] Copyright: 2025, American Chemical Society.

processing and microenvironment modeling, such as tumor-mimetic chips preserving native tissue architecture for on-chip EV secretion. These integrate combinatorial aptamer-induced dual-switch logic gates with connector probes targeting EpCAM/PD-L1, permitting real-time phenotypic subtyping of tumor/immune EVs within the TME and revealing immunotherapy-induced EV secretion dynamics (Fig. 3D).[73] Simultaneously, DNA nanomaterial-enhanced microfluidics employs λ-DNA scaffolds for simultaneous size-selective separation and multiplexed aptamer-based surface protein profiling of individual EVs. When coupled with machine learning classification, this resolves EV heterogeneity by identifying microvesicles as superior discriminators for breast cancer staging through HER2 expression correlation.[71] Moreover, a microfluidic-based DNA-enabled computational logic assay (DECLA) as another strategy for amplification-free detection, utilizing microfluidics and aptamer recognition. This method specifically detects extracellular PD-L1^{+} EVs while excluding soluble PD-L1 interference. DECLA employs a cholesterol-DNA probe embedding into EV membranes and a PD-L1-specific aptamer probe as dual inputs. A designed connector, stabilized by its secondary structure, activates only upon co-binding both probes. This activation mechanism rejects hybridization with soluble PD-L1. Consequently, target EVs are captured on streptavidin-functionalized herringbone-patterned microchannels and quantified *via* anti-CD63 labeling.[72] Exemplifying the power of programmable DNA nanostructures, the dual-protein logic profiling framework nucleic acid (DP-FNA) represents a sophisticated class of DNA nanomaterials engineered for high-fidelity EV analysis. This platform integrates two distinct aptamers into a rationally designed DNA framework that functions as a molecular computational device. Upon encountering individual EVs, the DP-FNA device performs quantitative assessment of relative target protein expression ratios (*e.g.*, CD63/EpCAM or EpCAM/CD63) through a retention-based logical profiling mechanism intrinsic to its nanostructure. Critically, the spatial organization of aptamers within the DNA framework enables Boolean-like operations – where retention signals depend on combinatorial biomarker expression patterns rather than absolute EV concentration. This design fundamentally decouples detection accuracy from sample variability, overcoming a key limitation of conventional single-aptamer assays (Fig. 3E).[70]

4.2. DNA-assisted signal amplification strategies

4.2.1. Enzyme-free catalytic amplification strategies. The described signal amplification strategies for exosome detection predominantly leverage DNA nanotechnology, with catalytic hairpin assembly (CHA), hybridization chain reaction (HCR), and other innovative DNA-based mechanisms constituting the primary classification frameworks. CHA-based systems are exemplified by methodologies employing proximity-induced catalytic cross-hybridization of hairpin probes to form three-way DNA junctions (3-WJ) that drive autocatalytic amplification, significantly enhancing sensitivity for subpopulation analysis.[74] Similarly, aptamer-initiated CHA (AICHA) exploits aptamer-target binding to trigger cascading hairpin openings, generating amplified fluorescence signals with exceptional sensitivity (Fig. 4A).[75] Furthermore, dual recognition-enabled amplification (DREAM) strategies utilize orthogonal aptamers to initiate proximity ligation, which subsequently activates CHA circuits coupled with self-propagating DNA cascades for ultrasensitive, multiplexed detection.[76] Another study introduced a Programmable Isothermal Cascade Keen Enzyme-free Reporter (PICKER) platform that integrated bivalent aptameric recognition of EpCAM and CD63 with CHA-mediated signal amplification, enabling precise quantification of circulating small EV (csEV) abundance within total small EV (tsEV) populations.[77]

HCR amplification strategies are extensively implemented, characterized by enzyme-free, toehold-mediated sequential hybridization events that yield extended DNA duplexes. These include systems where membrane-inserted cholesterol-modified DNA probes initiate HCR cascades, substantially increasing enzyme loading for downstream metallization-based signal transduction.[78] HCR is also integrated into dual-amplification architectures, such as electrochemiluminescence biosensors combining DNA bio-barcodes with HCR to generate elongated hemin-incorporated DNA nanostructures for robust signal enhancement.[79] Branched HCR (bHCR) further augments amplification efficacy by constructing intricate DNA networks on SERS-active substrates, creating dense hotspots for single-exosome detection.[80] HCR-based amplification concurrently increases the hydrodynamic diameter of single EV to be beyond 500 nm and recruits multiple fluorophores per probe, thereby markedly intensifying the fluorescence signal emanating from the sparse surface marker molecules. These combined effects render single EVs resolvable on standard flow cytometers and substantially facilitate multiplexed phenotyping of the same vesicle (Fig. 4B).[81]

Beyond CHA and HCR, alternative DNA amplification paradigms are employed. These encompass modular solid-phase peptide synthesis for precise valency control of SERS reporters, enabling stoichiometrically optimized labeling.[82] DNA cascade reactions achieve individual EV nanoencapsulation (DCR-IEVN) into large flower-like nanostructures, facilitating flow cytometric analysis without prior isolation.[83] Additionally, molecular computing strategies utilize aptamer-encoded EV surfaces with toehold-extended DNA aptamers executing AND-logic operations for multiplexed biomarker discrimination.[84] These diverse DNA technologies collectively underpin ultrasensitive, clinically translatable platforms for exosome-based diagnostics.

4.2.2. Enzyme catalytic amplification strategies. DNA nanotechnology provides a versatile foundation for engineering sophisticated biosensors targeting EVs, enabling ultrasensitive detection through programmable molecular circuits and nanostructures. CRISPR-Cas systems, predominantly Cas12a, are frequently integrated with DNA nanodevices to achieve exponential signal amplification *via trans*-cleavage activity. These platforms often employ proximity-driven DNA assembly, such as dual recognition probes ensuring co-localization on target EVs through specific surface biomarkers, to initiate cascading reactions. For instance, CHA amplification followed by CRISPR-Cas12a activation generates robust signals for breast cancer EV subtyping and staging,[85] while immunomagnetically

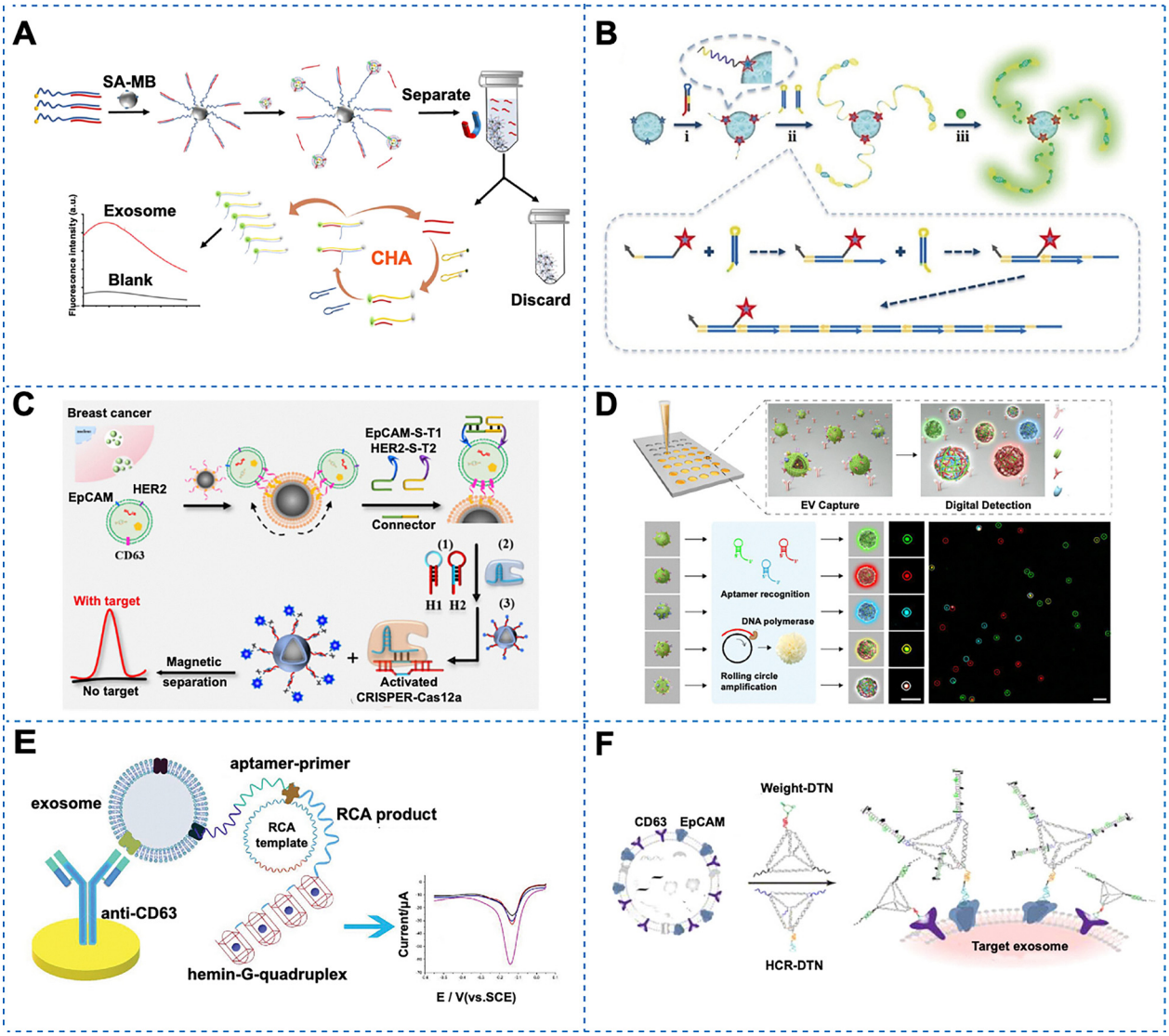

Fig. 4 DNA-assisted signal amplification strategies. (A) Aptamer-initiated catalytic hairpin assembly fluorescence assay for EV detection. Reproduced with permission.[75] Copyright: 2022, American Chemical Society. (B) HCR-based amplification for EV detection. Reproduced with permission.[81] Copyright: 2018, John Wiley and Sons. (C) CRISPR-based homogeneous electrochemical strategy for NearZero background detection of breast cancer EVs *via* fluidity-enhanced magnetic capture nanoprobe. Reproduced with permission. Reproduced with permission.[90] Copyright: 2025, American Chemical Society. (D) Localized fluorescent imaging of multiple proteins on individual EVs using rolling circle amplification for cancer diagnosis. Reproduced with permission.[99] Copyright: 2020, John Wiley and Sons. (E) A sensitive apt sensor based on a hemin/G-quadruplex Assisted signal amplification strategy for electrochemical detection of EVs. Reproduced with permission.[104] Copyright: 2019, John Wiley and Sons. (F) Fast and specific enrichment and quantification of cancer-related EVs by DNA-nanoweight-assisted centrifugation. Reproduced with permission.[110] Copyright: 2022, American Chemical Society.

enriched EVs trigger CRISPR-mediated fluorescence *via* programmable DNA circuits for lung cancer-derived EV PD-L1 quantification.[86] DNA-based AND-gate probes, activated by dual-aptamer proximity hybridization on EVs co-expressing markers like CD63 and VEGF, initiate autocatalytic exponential amplification circuits *via* CRISPR-Cas12a, significantly enhancing diagnostic specificity.[87] High-throughput profiling leverages dual-capture DNA nanotechnology (antibodies and switchable sgRNA-aptamer constructs) combined with Cas9-nickase proximity cleavage and polymerase-driven G-quadruplex assembly for multiplexed EV surface marker detection.[88] Furthermore, allosteric DNA probes recognizing EVs directly activate dual-cycle amplification cascades producing CRISPR RNA, enabling wash-free, linear quantification with sub-picomolar sensitivity,[89] and homogeneous electrochemical biosensors utilize AND-gate CHA with CRISPR-powered *trans*-cleavage of magnetic signaling reporters for near-zero background detection of breast cancer EVs (Fig. 4C).[90]

Polymerase-driven amplification, particularly rolling circle amplification (RCA), exploits DNA nanotechnology for efficient signal generation. Aptamer-mediated target recognition cyclizes padlock DNA probes, initiating branched RCA (BRCA) with fluorescent readouts for gastric cancer exosome detection.[91] Dual-aptamer proximity ligation assays (PLA) on

EV membranes generate DNA ligation products that template RCA, enabling ultrasensitive quantification of tumor-derived EV PD-L1 when coupled with droplet digital PCR (ddPCR)[92] or specific dual-positive subpopulations like $EpCAM^+/PD\text{-}L1^+$ T-EVs without purification.[93] Spatial multiplexing is achieved using DNA-functionalized, size-encoded microbeads segregated in microfluidic chips; *in situ* RCA on these beads allows simultaneous detection of six distinct tEV phenotypes.[94] Terminal deoxynucleotidyl transferase (TdT)-mediated DNA polymerization, triggered by aptamer sandwich assembly within functionalized nanochannels, provides localized amplification for cancer exosome detection.[95] RCA scaffolds also facilitate ultrasmall gold nanoparticle aggregation for single-particle ICP-MS readouts of tumor EVs,[96] and RCA-assisted flow cytometry enables multiplexed surface protein profiling on individual exosomes.[97] For Alzheimer's diagnosis, RCA on immunomagnetic beads quantifies enriched EV biomarkers captured *via* a DNA-aptamer-functionalized microfluidic chip.[98] Crucially, DNA nanotechnology enables single-EV resolution: localized RCA on antibody-captured EVs generates discrete fluorescent signals for digital multiplexed protein profiling (DPPIE), revealing diagnostically superior heterogeneity patterns (Fig. 4D).[99]

DNAzyme-based strategies utilize catalytic DNA nanostructures for signal modulation. A dual-control microchip employs DNA amplification cascades (likely involving DNAzyme components) coupled with electrokinetic enrichment and SERS for rapid, portable exosome detection.[100] Visual detection platforms integrate dual-recognition DNA probes with G-quadruplex DNAzymes that catalyze the etching of Au@Ag nanorods.[101] Conversely, signal quenching leverages DNA nanotechnology: binding-induced release of DNA triggers unwinds G-quadruplex/hemin DNAzyme structures *via* polymerase/endonuclease recycling, causing measurable signal attenuation for amplification-free sEV detection.[102] Electrochemical biosensors implement dual-aptamer AND-logic gates with cyclic enzymatic amplification (potentially involving DNAzymes) for specific sEV identification.[103] Based on the catalytic properties of G-quadruplex DNAzyme, a label-free electrochemical aptasensor was developed for the specific detection of gastric cancer exosomes. This platform employs an anti-CD63 antibody-modified gold electrode for generic exosome capture, coupled with a gastric cancer-specific aptamer linked to a primer sequence complementary to a circular G-quadruplex template. Upon recognition of target exosomes, the aptamer-primer complex triggers rolling circle amplification (RCA), generating multiple tandem G-quadruplex units. These RCA products self-assemble into catalytic G-quadruplex/hemin DNAzyme structures, which subsequently catalyze the reduction of hydrogen peroxide (H_2O_2) to produce a measurable electrochemical signal. The intrinsic catalytic activity of the DNAzyme enables sensitive and specific detection of gastric cancer exosomes, achieving a linear response from 4.8×10^3 to 4.8×10^6 particles mL^{-1} and a detection limit of 9.54×10^2 particles mL^{-1} (Fig. 4E).[104]

Other enzymatic strategies integrated with DNA nanotechnology address multiplexing challenges. A magnetically driven tandem chip uses cyclic SERS tags released *via* exonuclease I digestion (enzymatic recycling) to amplify signals for simultaneous quantification of six breast cancer EV biomarkers.[105] Membrane-functionalized sensing exploits bivalent cholesterol-modified RNA–DNA hybrid duplexes that insert into EV bilayers; duplex-specific nuclease (DSN) cleavage then releases amplifiable RNA signals, eliminating soluble protein interference.[106]

Collectively, DNA nanotechnology, through programmable probes, circuits, nanostructures, and amplification cascades, enables highly sensitive, specific, and multiplexed EV analysis, advancing liquid biopsy applications for cancer subtyping, staging, therapy monitoring, and neurodegenerative disease diagnosis.

4.2.3. DNA nanostructures-based amplification strategy. Programmable DNA nanostructures serve as precision-engineered scaffolds for enhanced EV analysis through spatial organization of recognition elements and signal amplification modules. Signal amplification was realized through a branched DNA structure, enabling quantification of the co-expression of eight outer proteins (integrins, tetraspanins) and four inner (heat shock, endosomal, inner leaflet) proteins.[107] Tetrahedral DNA nanostructures (TDNs) functionalized with dual-specificity aptamers against HER2 and CD63 enable targeted enrichment and detection of HER2-positive EVs (HEVs) from clinical samples, revealing significantly elevated HEV levels in HER2-positive breast cancer patients (mean: 4.737 U μL^{-1}) *versus* healthy controls (4.144 U μL^{-1}, $P < 0.0001$) with progressive concentration gradients correlating to HER2 expression levels.[108] Similarly, trivalent aptamer-conjugated TDNs (triApt-TDN) spatially organize MUC1-specific aptamers on plasmonic substrates to capture gastric cancer exosomes, where trigger aptamers initiate branched hybridization chain reaction (bHCR). This assembles gold nanoparticle networks generating dense surface-enhanced Raman scattering (SERS) hotspots, achieving single-exosome sensitivity in clinical serum within 60 minutes and effectively discriminating gastric cancer patients.[86] Complementary to rigid frameworks, rolling circle amplification (RCA)-synthesized DNA nanoflowers (DFs) create multivalent microspheres with spatially ordered EpCAM aptamers. These flexibly adapt to EV membrane topology, significantly improving capture efficiency (92.4 ± 3.1%) over monovalent constructs (68.7 ± 5.2%).[109] Critically, DFs' optical transparency permits direct on-structure quantification of captured EVs *via* hydrophobic signaling assembly, demonstrating superior diagnostic accuracy (88.3%) *versus* conventional biomarkers like carcinoembryonic antigen (CEA, 76.7%) in clinical cohorts. Concurrently, a dual-TDN strategy employs one nanostructure to cross-link target exosomes for efficient low-speed centrifugal enrichment, while another initiates hybridization chain reaction (HCR) for signal amplification. This approach achieves detection limits of 1.8×10^2 exosomes per μL for MCF-7-derived EVs representing 1000-fold higher sensitivity than ELISA-while eliminating interference from soluble proteins through multi-protein recognition (Fig. 4F).[110]

Collectively, these DNA nanostructures overcome critical limitations in EV analysis: TDNs and DFs enable multivalent binding that enhances capture specificity and efficiency;[108–110]

integrated amplification strategies (bHCR, HCR, RCA) provide ultrasensitive detection down to single-EV resolution;[86,109,110] and clinical validations demonstrate robust diagnostic capabilities for cancer subtyping (*e.g.*, HER2-positive breast cancer,[108] gastric cancer[86]) and biomarker quantification.[109] The spatial control afforded by DNA nanotechnology thus establishes a transformative platform for membrane protein profiling, resolving EV heterogeneity and advancing non-invasive cancer diagnostics.

4.3. Glycoprotein detection

Glycosylation, a major co- and post-translational modification (PTM), critically regulates the structure, sorting, and function of proteins within EVs. The disease-specific alteration of glycoproteins on EV surfaces generates unique "glycosignatures" that serve as powerful biomarkers for diagnosis, prognosis, and therapeutic monitoring.[45,111] Mucin 1 (MUC1) is a transmembrane glycoprotein characterized by an extensively *O*-glycosylated extracellular domain.[112] In healthy tissues, the primary *O*-glycans consist of *N*-acetylgalactosamine (GalNAc), *N*-acetylglucosamine (GlcNAc), and galactose. These heavily glycosylated structures are negatively charged and undergo oligomerization to establish a dense mucinous layer. This layer confers anti-adhesive properties and protects the underlying epithelium from desiccation, pH fluctuations, and pathogenic colonization. But in breast epithelial cancers, MUC1 is markedly overexpressed and exhibits aberrant glycosylation characterized by truncated *O*-glycans.[113] EVs from metastatic Hepatocellular Carcinoma (HCC) cells carry the glycoprotein nidogen-1 (NID1). Levels of NID1-containing EVs and TNF receptor 1 (TNFR1) in serum correlate with advanced HCC stage and promote lung metastasis, suggesting their use as non-invasive biomarkers.[114] Ascites-derived exosomes from pancreatic cancer (PC) patients contain highly sialylated CD133. Higher levels of glycosylated CD133 correlate with poorer survival, suggesting its use as a biomarker for advanced disease.[115]

Detection methodologies based on DNA nanotechnology for these specific glycoforms can be broadly categorized based on the presence or absence of signal amplification. Non-amplified approaches directly visualize or quantify the target glycoproteins. For instance, a dual-labeling strategy integrating protein-specific aptamer tagging with metabolic glycan labeling enables *in situ* visualization of glycosylation on target EV proteins, such as PD-L1, through intramolecular fluorescence resonance energy transfer (FRET), facilitating spatial mapping and functional investigation (Fig. 5A).[116] Similarly, a glycosyl-imprinted electrochemiluminescence (ECL) sensor exploits molecularly imprinted polymers (MIPs) for high-specificity capture of EVs and dual-aptamer labeling for potential-resolved detection of coexisting glycoprotein biomarkers (*e.g.*, PD-L1 and MUC1) without enzymatic or nucleic acid

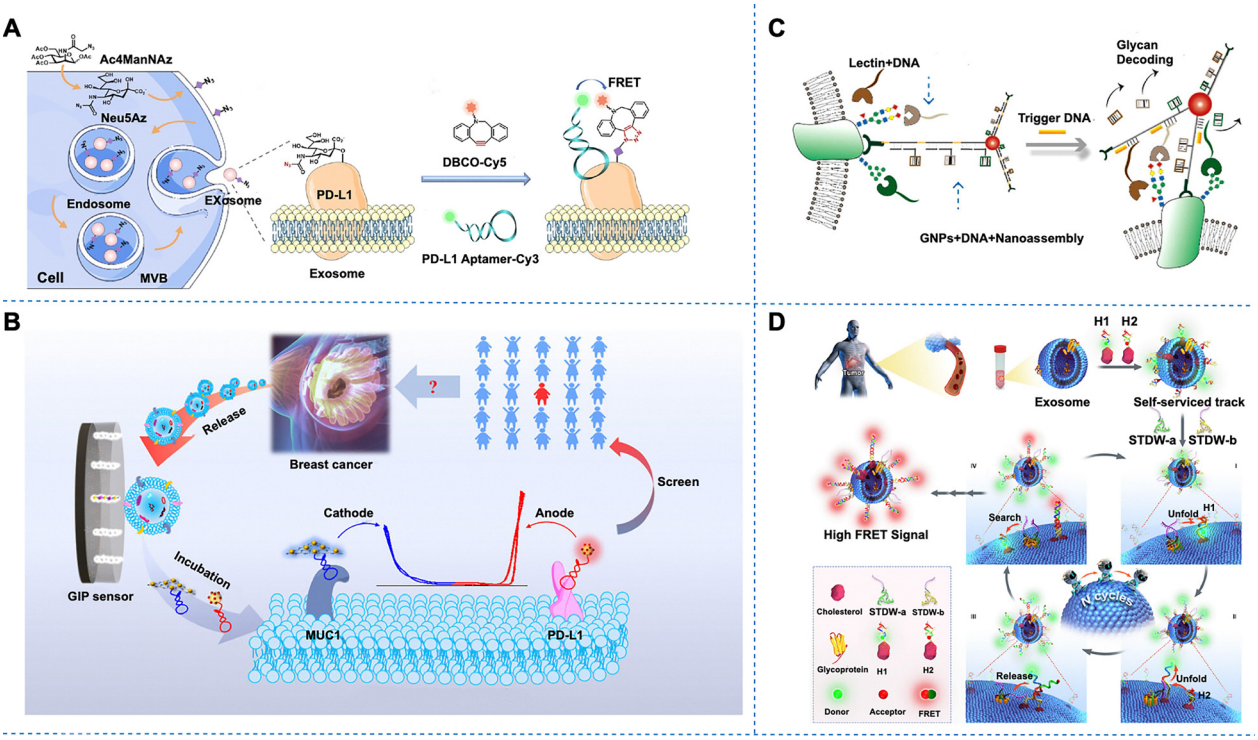

Fig. 5 Glycoprotein detection. (A) Non-amplified approaches directly visualize or quantify the target glycoproteins based on spectrum. Reproduced with permission.[116] Copyright: 2021, John Wiley and Sons. (B) A glycosyl-imprinted sensor used for accurate classification and quantification of breast cancer-derived exosomes by electrochemiluminescence detection. Reproduced with permission.[117] Copyright: 2025, American Chemical Society. (C) A strand displacement cascade signal-amplified strategies Reproduced with permission.[118] Copyright: 2023, American Chemical Society. (D) A self-serviced-track 3D DNA walker signal-amplified strategies. Reproduced with permission.[119] Copyright: 2022, John Wiley and Sons.

amplification (Fig. 5B).[117] In contrast, signal-amplified strategies enhance detection sensitivity for low-abundance targets. One approach utilizes DNA-encoded affinity ligands, where dual DNA tags selectively label target proteins and their glycans. Sequence-programmable manipulation of these tags and a spatial proximity-activated DNA logic gate liberate glycan-representative DNA strands *via* a strand displacement cascade. This cascade enables indirect signal amplification, as the released DNA barcodes are subsequently quantified using highly sensitive techniques like qPCR, allowing multiplexed glycoform analysis across EV subpopulations (Fig. 5C).[118] Another conceptually distinct amplified method employs a self-serviced-track DNA walker (STDW) platform. This system leverages split aptamer recognition of EV glycoproteins to initiate CHA-powered autonomous DNA walking operations directly on the captured exosome surface, acting as a three-dimensional molecular track. This enzymatic amplification process provides wash-free, highly sensitive quantification of tumor EVs in complex biofluids (Fig. 5D).[119]

5. DNA nanotechnology-enabled EV nucleic acid detection

EVs encapsulate diverse nucleic acids (primarily miRNAs, but also mRNAs, lncRNAs, DNA fragments) that serve as crucial functional molecules and disease biomarkers. Detection methodologies are broadly classified into two principal categories: membrane lysis of EVs followed by analysis, and *in situ* detection. Detection challenges include extremely low abundance, susceptibility to degradation, and the need for high specificity. DNA-based technologies offer robust solutions to these constraints through programmable probe design and enzymatic or enzyme-free signal amplification.

5.1. EV nucleic acid detection after lysis

5.1.1. Enzyme-free catalytic amplification strategies. Several electrochemical biosensors exploit sophisticated catalytic hairpin assembly (CHA) circuits, including step polymerization CHA (SP-CHA) generating T-shaped concatemers for EVs miR-181 detection with a femtomolar (fM) limit of detection (LOD),[120] and turbo-like localized CHA (TL-CHA)[121] or dominotype localized CHA (DT-LCHA)[122] leveraging DNA nanowires and gold nanoparticles (AuNPs) to spatially confine reactions, achieving attomolar (aM) sensitivity for sEV-miRNAs like miR-1246 within 20–30 minutes. These localized CHA strategies enhance collision efficiency, enable domino effects, and facilitate loading of numerous signal reporters (*e.g.*, RuHex), collectively improving signal-to-noise ratios.[121,123] Parallel developments involve novel hybridization chain reaction (HCR) formats; a microfluidic chemiluminescence platform integrates exosome capture, Y-shaped arrays, HCR, and poly-HRP catalysis for multiplexed, femtomolar detection of EVs miR-21 and miR-155 (Fig. 6A),[122] while a dumbbell HCR (DHCR) coupled with strand displacement amplification (SDA) achieves attomolar sensitivity for EVs miRNA by forming compact DNA nanostructures.[124] Beyond cancer diagnostics (*e.g.*, gastric cancer,[121,123] coronary heart disease[120]), enzyme-free amplification, exemplified by locked hairpin DNA-functionalized Au nanoprobes enabling target-triggered hairpin assembly and fluorescence signal generation, proves effective for multi-miRNA profiling in urinary sEVs for systemic lupus erythematosus (SLE) diagnosis and stratification (Fig. 6B).[125]

5.1.2. Enzyme catalytic amplification strategies. Based on the current literatures, enzyme-mediated signal amplification strategies for ultrasensitive detection of EV-derived nucleic acids can be classified into the following categories.

CRISPR-Cas nucleases are extensively employed for their dual cleavage activities and high specificity. Systems integrating rolling circle amplification (RCA) with CRISPR-Cas9 (RACE) achieve single-base resolution through dual recognition (padlock probe ligation and PAM-triggered cleavage), enabling multiplexed EV-miRNA quantification with clinical validation in lung cancer diagnosis.[126] The EXTRA-CRISPR platform further innovates by unifying *cis*-cleavage (exponential RCA amplification) and *trans*-cleavage (signal detection) of Cas12a in a one-pot isothermal assay, attaining single-digit femtomolar sensitivity for EV-miRNAs in pancreatic cancer plasma within 20 minutes to 3 hours.[127] Cas13a-based systems excel in complex scenarios: CRISPR/Cas13a leverages machine learning to analyze fecal EV-miRNA signatures (FEVOR) for colorectal cancer diagnostics (97.4% accuracy),[128] while stem-loop-enhanced Cas13a in the "Logic-Measurer" system accelerates *trans*-cleavage kinetics *via* optimized RNA hairpin structures, enabling logic-gated multiplexed miRNA detection for breast cancer staging.[129] DNA walker-mediated CRISPR activation also proves effective, where 3D DNA walkers convert exomiRNAs into DNA activators to trigger Cas12a *trans*-cleavage, achieving 20.42 fM sensitivity for osteoporosis diagnosis.[130] For mRNA analysis, Cas13-initiated replication (SCOPE) combines CRISPR recognition with polymerase-driven amplification, detecting tumor mutations in EVs at sub-attomolar levels (Fig. 6C).[131]

DNAzymes serve as catalytic nucleic acids for rapid, enzyme-free amplification. Mg^{2+}-dependent DNAzymes on gold nanoparticles minimize false positives *via* dithiol anchoring, detecting EV PD-L1 RNA at 50 fM in 8 minutes.[132] Similarly, inorganic nanoflare-DNAzyme walkers on AuNPs cleave fluorophore-labeled substrates upon miRNA activation, allowing simultaneous femtomolar-level detection of bladder cancer EV-miRNAs.[133] The nucleic acid lock (NAL) cycle employs target-triggered DNAzyme cleavage to release initiator strands, driving hybridization chain reaction (HCR) and electrochemical signal amplification for lung adenocarcinoma EV-miRNA detection (26 aM limit) (Fig. 6D).[134]

Polymerase-driven isothermal amplification strategies circumvent thermal cycling. Exponential amplification reaction (EXPAR) reactivates Cas9/sgRNA complexes *via* miRNA-triggered DNA production, enabling visual detection of EV miR-21 at 3×10^3 particles per mL for point-of-care cancer screening.[135] Microfluidic integration of EXPAR allows multiplexed EV-miRNA profiling in 90 minutes using an IoT-based reader.[136] Rolling circle amplification (RCA) is leveraged in encoded hydrogel particles for absolute EV-miRNA quantification (LOD: 2.3 zmol) (Fig. 6E),[137] while on-chip RCA combined with molecular beacons enables

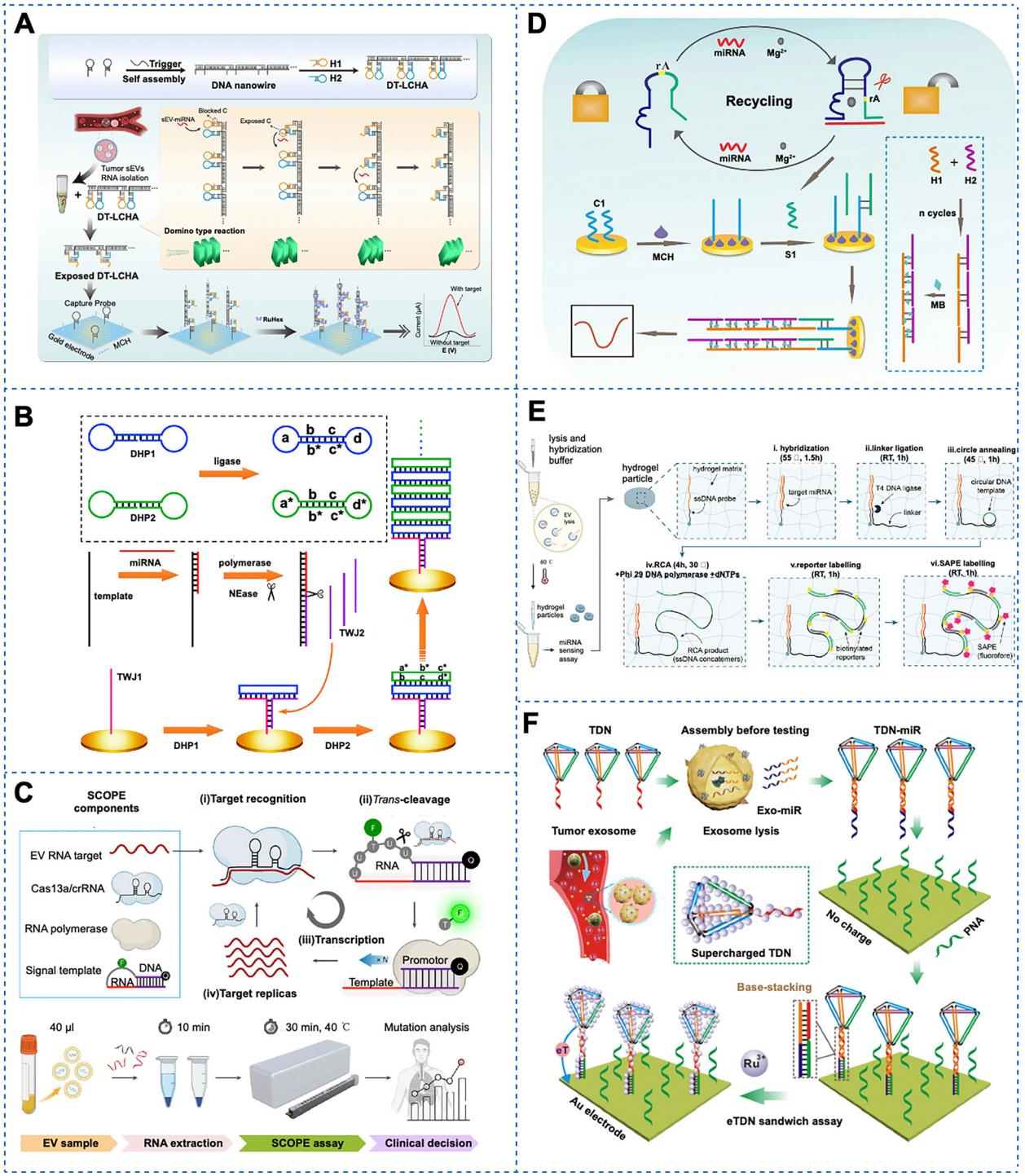

Fig. 6 Enzyme catalytic amplification strategies. (A) sEV-miRNA detection based on domino-type localized catalytic hairpin assembly. Reproduced with permission.[122] Copyright: 2023, Springer Nature. (B) Dumbbell hybridization chain reaction based electrochemical biosensor for EV miRNA detection. Reproduced with permission.[125] Copyright: 2020, American Chemical Society. (C) Amplifying mutational profiling of EV mRNA with SCOPE. Reproduced with permission.[131] Copyright: 2024, Springer Nature. (D) Target-triggered DNAzyme for detection of EV miR-4732-5p. Reproduced with permission.[134] Copyright: 2024, Springer Nature. (E) Quantitative and multiplex detection of EV MicroRNA *via* rolling circle amplification within encoded hydrogel microparticles. Reproduced with permission.[137] Copyright: 2022, John Wiley and Sons. (F) Ultrasensitive EV MicroRNA detection with a supercharged DNA framework nanolabel. Reproduced with permission.[146] Copyright: 2021, American Chemical Society.

"turn-on" fluorescence detection of neutrophil EV-miRNAs for gastric cancer diagnosis.[138] RT-dPCR-based molecular quantification of EV-derived messenger ribonucleic acid (mRNA) was enabled by a lipid labeling and click chemistry EV capture platform ("Click Beads"), which provides rapid, efficient purification critical for downstream analysis.[139]

Integrated enzymatic-nanomachine systems synergize multiple mechanisms. A 3D DNA nanomachine stabilized by Pt–S bonds couples with liposome nanocarriers for homogeneous electrochemical detection of EV miRNA in plasma, minimizing background noise.[140] Localized DNA cascade displacement reactions (L-DCDR) with DNA nanosheets achieve enzyme-free electrochemical sensing at 65 aM, exploiting toehold-mediated strand displacement for high signal-to-noise ratios.[141]

These strategies collectively achieve exceptional sensitivity (aM-zmol), single-nucleotide specificity, and point-of-care compatibility. Clinical validations across diverse cohorts-including cancers (lung,[126,134] pancreatic,[127] colorectal,[128,131] bladder,[133] gastric[138]) and osteoporosis[130]-highlight their translational potential for liquid biopsy diagnostics.

5.1.3. DNA nanostructures-based amplification strategy. DNA nanostructures, particularly tetrahedral DNA frameworks (TDNs), serve as precision-engineered scaffolds enabling significant advancements in biosensing platforms. These frameworks facilitate high-density anchoring of biorecognition elements through their spatially controlled vertices, enhancing probe accessibility and hybridization efficiency. In electrochemiluminescent (ECL) systems, TDNs act as ''bottom-up'' anchor bioprobes to optimize the *trans*-cleavage activity of CRISPR/Cas12a, while simultaneously supporting nanozymes (*e.g.*, TCPP-Fe@HMUiO@Au) to amplify signals through augmented catalytic sites and mass transfer.[142] Alternatively, TDN probes can initiate template-independent DNA hydrogelation on surfaces,[143] leveraging the hydrogel's high dielectric constant to dramatically improve imaging ellipsometry sensitivity with tunable dynamic ranges *via* amplification cycle modulation. Dimeric framework nucleic acid (FNA) nanoplatforms further exemplify multifunctional DNA architectures.[144] One FNA unit functionalized with aptamers captures Evs, while a proximal FNA unit incorporates target-responsive Y-junctions for loading catalytic nucleic acid enzymes (*e.g.*, hemin-modified SNAs). This spatial organization enables direct on-site ECL signal amplification without RNA extraction. For electrochemical sensing, tetrahedral DNA mediates cascade amplification through streptavidin-biotin binding, immobilizing hybridization chain reaction (HCR) products that adsorb electroactive reporters.[145] Crucially, the supercharged nature of TDNs permits stoichiometric adsorption of signaling molecules (Fig. 6F),[146] and when combined with peptide nucleic acid (PNA) probes to minimize background, achieves ultrasensitive ''assembly-before-testing'' detection. This exploits base-stacking effects to stabilize target-conjugated sandwich complexes on electrodes.

In summary, these DNA frameworks, including TDNs,[142,143,145,146] FNAs,[144] and hydrogel-forming tetrahedrons,[143] provide modular, stable, and electrostatically tunable interfaces. They enable enzyme-free amplification,[145,146] spatial control for reaction optimization,[142,144] and direct signal enhancement, pushing detection limits to aM-fM levels[142,146] while maintaining specificity in complex biological matrices.[143,144,146] This structural paradigm underscores the critical role of nucleic acid nanotechnology in realizing ultrasensitive, clinically translatable EV miRNA diagnostics.

5.2. Detection of EV nucleic acid *in situ*

Traditional lysate-based detection methods were prone to false negative results due to cargo loss during sample preparation while also eliminating cell-specific information within individual EVs.[147,148] *In situ* nucleic acid detection of EVs primarily falls into two categories: one approach relies on membrane fusion between probe-loaded liposomes and EVs, while the other is based on transmembrane penetration of probes across the EVs membrane.

5.2.1. Membrane fusion. EV-associated RNAs represent highly promising biomarkers for the early diagnosis of diseases and therapeutic monitoring. However, conventional detection methods relying on EV enrichment, RNA extraction, and qRT-PCR are often time-consuming, costly, and complex. To overcome these limitations, innovative strategies leveraging membrane fusion between engineered probes and target EVs have emerged, enabling rapid, direct, and sensitive *in situ* RNAs analysis without prior isolation or extraction. These approaches can be broadly categorized based on the incorporation of signal amplification.

Non-amplified fusion strategies facilitate rapid detection by inducing direct content mixing between probe vesicles and EVs upon recognition. Key recognition and fusion triggers include: DNA zipper constructs (ZDCs and cZDCs) mediating specific vesicle-exosome fusion for fluorescence-based miRNA detection within 30 minutes using molecular beacons (MBs) encapsulated in lipid vesicle probes, enabling tumor exosome distinction *via* flow cytometry.[149] Encoded-targeted-fusion beads (ETFBs) utilize combinatorial fluorescence/size barcodes and surface aptamers for selective tEV fusion and multiplexed miRNA profiling directly from minute plasma volumes (2 μL) using flow cytometry, achieving high diagnostic accuracy.[150] Virus-mimicking fusogenic vesicles (Vir-FVs) employ fusogenic proteins targeting sialic acid receptors for efficient exosome fusion and MB-based miRNA detection within 2 hours, allowing tumor exosome discrimination.[151] Charged liposomes (CLIPs) fused with EVs in microfluidic droplets (EV-CLIP) enable highly sensitive digital detection of EV RNA (miRNA/mRNA) from small plasma volumes (20 μμL), demonstrating excellent clinical performance for mutation detection.[152] Aptamer-mediated selective fusion (Apt-Fusion) exploits aptamers for rapid and selective tumor-derived EV fusion, allowing sensitive quantification of specific EV subpopulations (*e.g.*, PD-L1 + EVs) and correlation with disease burden using conventional flow cytometry.[153] Fusogenic nanoreactors (FNRs) decorated with hemagglutinin (HA) proteins achieve sialic acid-binding and fusion, encapsulating DNA-fueled molecular machines (DMMs) for direct, multiplexed EV miRNA detection within 30 minutes *via* a single mix-and-read step, significantly improving diagnostic accuracy through multi-miRNA panels.[154]

Amplified fusion strategies integrate signal amplification mechanisms within the fusion platform to achieve ultrasensitive detection. These include multifunctional magnetic vesicles incorporating virus-mimicking proteins for hepatogenic exosome-specific fusion and an internal cascade combining catalytic hairpin assembly (CHA) with CRISPR/Cas13a for highly sensitive, amplification-free miRNA detection directly within fused EVs, achieving low limits of detection (LOD ~ 125

particles per μL) for applications like drug-induced liver injury (DILI) diagnosis.[155] The liposome-mediated membrane fusion strategy for CRISPR/Cas13a transfection (MFS-CRISPR) delivers Cas13a components into EVs *via* fusion, enabling direct,

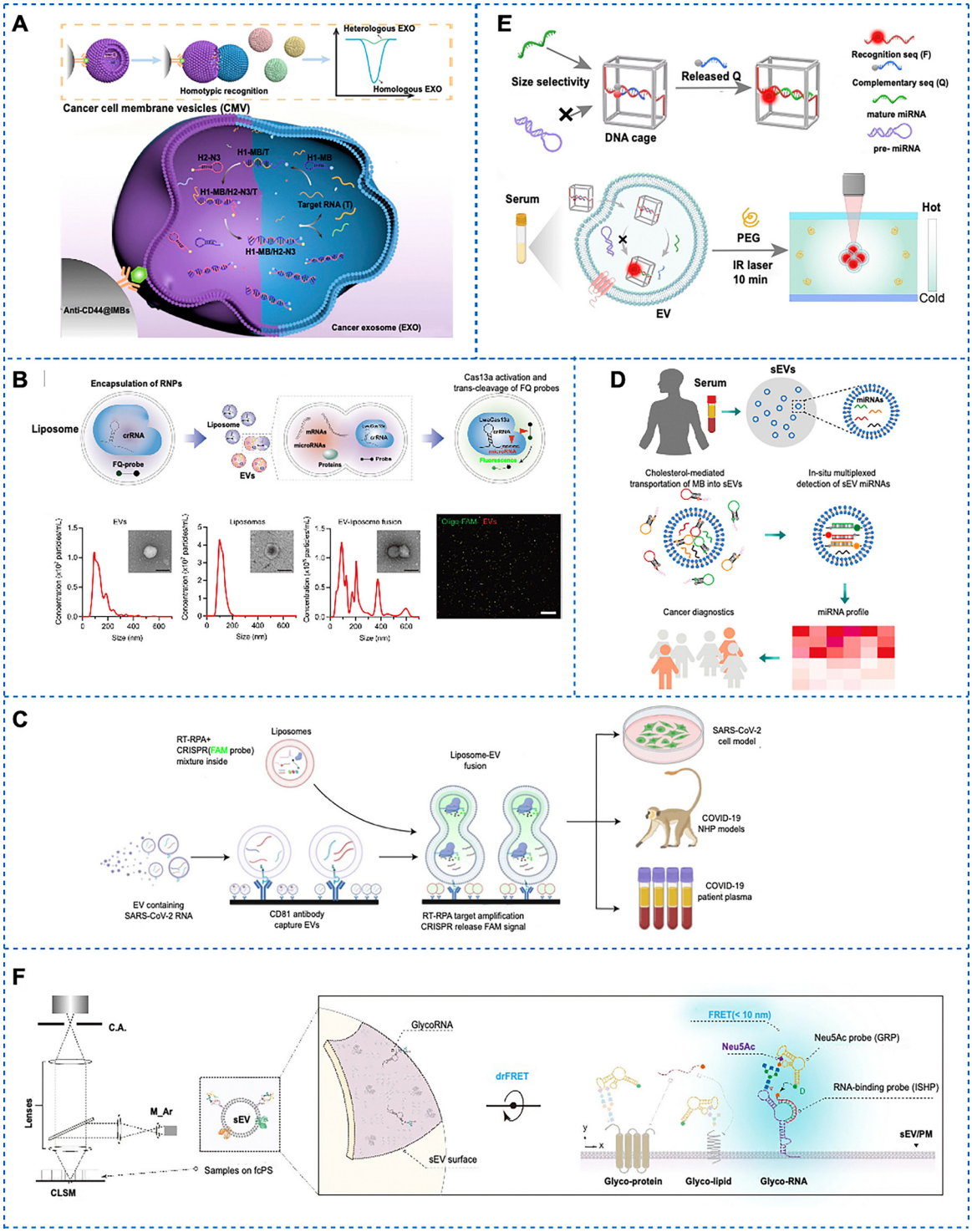

Fig. 7 Detection of EVs nucleic acid *in situ*. (A) Membrane fusion strategy based on enable homotypic recognition and fusion with phenotypically matched circulating EVs. Reproduced with permission.[158] Copyright: 2022, American Chemical Society. (B) CRISPR/Cas13a sensing components encapsulated in liposomes. Reproduced with permission.[159] Copyright: 2023, John Wiley and Sons. (C) Liposome-mediated detection of SARS-CoV-2 RNA-positive EVs in plasma. Reproduced with permission.[160] Copyright: 2021, Springer Nature. (D) Transmembrane molecular beacons strategy. Reproduced with permission.[163] Copyright: 2024, American Chemical Society. (E) A DNA Cage-Based transmembrane strategy. Reproduced with permission.[167] Copyright: 2023, John Wiley and Sons. (F) FRET imaging of glycoRNA on sEVs enabling sensitive cancer diagnostics. Reproduced with permission.[173] Copyright: 2025, Springer Nature.

sensitive (LOD ~ 1.2×10^3 particles per mL) quantification of EV miRNAs and analysis of EVs heterogeneity.[156] DNA logic-circuit-engineered protocells (liposomes) process EVs surface protein signals *via* AND, OR, and NOT gates to achieve highly selective fusion only with target EVs, followed by target miRNA-triggered walker probe amplification, enabling accurate tumor EVs miRNA detection in clinical samples.[157] Biomimetic vesicles, camouflaged with cancer cell membranes, enable homotypic recognition and fusion with phenotypically matched circulating EVs; encapsulated catalytic DNA machinery uses EVs RNA as an endogenous trigger for amplified electrochemical signaling, allowing sensitive subtyping and staging of breast cancer (Fig. 7A).[158] CRISPR/Cas13a sensing components encapsulated in liposomes are delivered into EVs *via* fusion, enabling extraction-free digital counting of specific miRNA-positive EVs (sensitivity down to 1×10^8 total EVs) and facilitating multiplexed protein-miRNA analysis within EV subpopulations (Fig. 7B).[159] A targeted fusion approach using reagent-loaded liposomes fused directly with plasma EVs captured SARS-CoV-2 RNA, enabling sensitive amplification and detection that extended the diagnostic window significantly beyond respiratory RT-qPCR in both non-human primates and pediatric patients (Fig. 7C).[160]

In summary, membrane fusion-based EV detection platforms offer significant advantages: elimination of EV isolation and RNA extraction steps, minimal sample volume requirements (often $\leq$ 40 μL), rapid processing times (30 minutes to 2 hours), compatibility with common readouts like flow cytometry, and direct *in situ* analysis preserving EV heterogeneity. While non-amplified methods provide speed and simplicity, amplified strategies achieve exceptional sensitivity and enable digital or multiplexed analysis. Both paradigms demonstrate high clinical accuracy in distinguishing disease states across various applications, including cancer diagnosis, subtyping, staging, and infectious disease monitoring, representing a transformative shift towards simpler, faster, and more reliable liquid biopsy tools.

5.2.2. Transmembrane DNA probes. While traditional lysate-based methods risk cargo loss and sacrifice single-EV information, *in situ* detection of EVs miRNAs has advanced significantly, particularly through transmembrane delivery of DNA-based probes. Initial approaches employed molecular beacons (MBs), where fluorescent hairpin oligonucleotides successfully quantified miRNA-21 within breast cancer EVs; permeabilization with streptolysin O enhanced probe entry and signal intensity, enabling specific cancer exosome detection in complex mixtures and serum.[161,162] Hydrophobic tether-conjugated MBs were later repurposed for fusion-free, multiplexed sEV miRNA detection (Fig. 7D),[163] achieving high diagnostic accuracy (83.3–100%) in clinical cohorts. To overcome limitations like fluorescence quenching and unwanted FRET within the confined EV space caused by probe collisions during Brownian motion, subsequent strategies utilized engineered framed nucleic acid architectures. These include cubic DNA nanocages (ncMBs) that leverage steric hindrance and electrostatic repulsion to prevent signal distortion, achieving an order-of-magnitude signal improvement over conventional MBs,[164] and double-accelerated DNA cascade amplifiers (DDCAs) exploiting spatial confinement within DNA nanocubes to enhance catalytic hairpin assembly (CHA) kinetics for sensitive FRET-based miRNA-21 imaging.[165] DNA tetrahedron probes achieved unprecedented single-copy miRNA imaging within intact EVs,[166] while DNA cage-PEG thermophoretic assays enabled selective mature miRNA detection (LoD: 2.05 fM) by excluding pre-miRNA interference (Fig. 7E).[167] Concurrently, gold nanoparticle (AuNP)-DNA composite nanoprobes emerged, offering efficient membrane penetration and integrated signal amplification. Examples include AuNPs functionalized with Raman reporters (Au@DTNB) for SERS-based *in situ* quantification (LOD: 0.21 fM),[168] dual-specificity logic gates driven by entropy-driven catalysis (EDC) on AuNPs for accurate liver cancer exosome classification *via* miR-21/miR-122 profiling,[169] nanoflare-conjugated AuNPs enabling thermophoretic enrichment (TSN) for PCR-comparable sensitivity in serum,[170] and nanoflare-CHA systems integrated with deep learning for automated, multi-miRNA analysis of single EVs using TIRF imaging.[171] Collectively, these transmembrane DNA probe strategies, spanning optimized molecular beacons,[161,163] structurally stabilized nucleic acid frameworks,[164–167] and multifunctional AuNP composites,[168–171] provide powerful, sensitive, and clinically translatable platforms for non-destructive *in situ* EV miRNA analysis, preserving vesicular integrity and single-EV heterogeneity crucial for liquid biopsy and cancer diagnostics.

In addition to the aforementioned unmodified nucleic acids, recent studies have identified glycosylated RNAs (glycoRNAs) as a novel class of membrane-associated molecules on small EVs (sEVs), where RNA is post-translationally modified with glycans such as *N*-acetylneuraminic acid (Neu5Ac). These glycoRNAs play critical roles in sEV-mediated cellular communication, including interactions with Siglec receptors and *P*-selectin, yet their study has been hindered by limitations in sensitive, spatial detection methods.[172] To address this, a dual-recognition Förster resonance energy transfer (drFRET) strategy was developed, leveraging two DNA probes: a glycan recognition probe (GRP) comprising a Neu5Ac-specific ssDNA aptamer conjugated to Cy3, and an *in situ* hybridization probe (ISHP) comprising a target-RNA-complementary ssDNA conjugated to Cy5 (Fig. 7F).[173] sEVs are first captured from minute biofluid volumes ($\geq$10 μL) using aptamer-functionalized beads, then incubated with both probes. FRET occurs only when simultaneous binding of GRP to Neu5Ac and ISHP to RNA brings the fluorophores within $\leq$10 nm proximity, enabling highly specific *in situ* imaging. The corrected FRET (cdFRET) signal, quantified *via* sensitized emission microscopy, correlates with glycoRNA abundance and exhibits a detection limit of 7.7×10^4 sEVs per mL. This approach validated glycoRNA presence on cancer-derived sEVs, revealed their direct binding to Siglec-10/11 and P-selectin, and demonstrated their functional role in sEV internalization-ablating surface glycoRNAs reduced cellular uptake by >69%. Clinically, drFRET achieved 100% accuracy in distinguishing cancer from non-cancer cases and 89% accuracy in multi-cancer typing using sEV glycoRNA profiles,

establishing it as a versatile platform for probing glycoRNA biology and advancing liquid biopsies.

6. Simultaneous detection of proteins and nucleic acids in EVs

The inherent heterogeneity and biological complexity of malignancies render reliance on single-class EV-associated biomarkers insufficient, necessitating multimodal biomarker approaches for precise cancer diagnosis and staging. Consequently, the development of cross-molecular biomarker panels integrating proteins and miRNAs constitutes a pivotal research frontier in EV-based diagnostics.[174–177] Rational biomarker selection must consider tissue-specific expression profiles, as tumor-derived EVs exhibit distinct molecular signatures, for instance, elevated EGFR, LG3BP, miR-21, and miR-210 in lung cancer-derived EVs *versus* enrichment of ANXA8 and miR-342 in breast cancer-derived EVs. Optimal biomarker combinations require molecular complementarity and co-localization within specific EV subpopulations.

Two principal paradigms guide biomarker panel selection: First, functional synergy prioritizes molecules that cooperatively drive oncogenic processes. In lung cancer, the EGFR/miR-21 panel exemplifies this principle: EGFR activates the PI3K/Akt pathway while miR-21 potentiates downstream signaling through PTEN suppression. Their cooperative action amplifies tumor progression, with combined detection significantly enhancing diagnostic accuracy compared to single-analyte assessment.[178,179] Second, regulatory reciprocity leverages molecules with interdependent regulatory relationships. For breast cancer-derived EVs, miR-342 directly represses ANXA8 translation while ANXA8 transcriptionally downregulates miR-342. This antagonistic regulation establishes a diagnostically informative expression ratio that improves discrimination between malignant and healthy states.[179,180] Compared to single-analyte approaches, cross-type biomarker panels integrate multidimensional molecular information from EVs. This captures key pathogenic cascades while compensating for inherent limitations in the sensitivity or specificity of individual biomarkers.[181] The integrative strategy thus enables more precise early cancer detection and longitudinal monitoring of disease progression through EV analysis.

The concurrent detection of proteins and nucleic acids within EVs is essential for comprehensive biomarker profiling in liquid biopsy, yet remains technically challenging due to spatial compartmentalization, heterogeneity, and low target abundance. Advanced methodologies address this through two primary strategies: membrane fusion-based approaches preserving EV integrity *versus* lysis-based techniques enabling maximal signal recovery.

Non-destructive membrane fusion strategies facilitate *in situ* co-detection by delivering probes across intact membranes. Several DNA-based strategies have been reported. Breast cancer-derived EVs were identified *via* flow cytometry using a dual-targeting strategy. Surface PD-L1 protein was recognized by a fluorophore-conjugated aptamer, while intravesicular miR-21 was detected using a conformation-switching molecular beacon (MB-21) featuring a hairpin-quenched fluorophore that activates upon miRNA hybridization.[182] Liu *et al.* reported Fusogenic vesicles encapsulating molecular beacons for internal miRNAs paired with quantum dot-labeled aptamers targeting surface proteins (*e.g.*, CD81, EphA2, CA19-9) in microfluidic devices.[183] CRISPR-Cas powered systems combining antibody-DNA conjugates (Cas12a) for surface proteins with vesicle-liposome fusion (Cas13a) for internal miRNAs in digital microfluidic arrays (ddSEE) (Fig. 8A).[184] Single-particle interferometry (SPIRFISH) coupling interferometric protein detection with single-molecule FISH for internal genomic RNA in HIV virions/EVs.[185] Biochip enrichment (BARA) enabling *in situ* antigen and RNA co-detection at single-particle resolution.[186] These approaches maintain vesicle topology, allowing spatial correlation of surface markers with intravesicular nucleic acids.

Lysis-dependent strategies achieve ultra-sensitive co-detection by liberating intravesicular contents for amplification: Antibody-DNA probes converting target proteins (*e.g.*, CD63, GPC-1, HER2) into amplifiable double-stranded DNA signals, coupled with qRT-PCR for released RNAs (miRNAs, mRNAs) in the Co-PAR platform (Fig. 8B).[187] Dual-cycling nanoprobes (DCNP) using gold nanoparticle-assembled DNA machines for synchronized signal amplification of surface PD-L1 and lysed miR-21.[188] Aptamer-PCR platforms quantifying surface proteins (*e.g.*, PD-L1 *via* aptamer-PCR) and internal RNAs (*e.g.*, IDO1 mRNA *via* RT-PCR) post-lysis.[189] These methods prioritize sensitivity through nucleic acid amplification cascades, transforming both protein and RNA targets into quantifiable DNA signals. Therefore, these platforms exploit nucleic acid engineering, including aptamers, CRISPR guide RNAs, hybridization probes, and amplification circuits, to overcome spatial segregation and achieve multiplexed protein-nucleic acid co-detection. This dual-target capability significantly enhances diagnostic precision by capturing complementary molecular signatures within individual EVs.

7. Challenges and future perspectives

DNA-based detection technologies are fundamentally reshaping the analytical landscape for EVs, offering unparalleled capabilities for sensitive, multiplexed, and single-particle analysis. The core strength of these technologies lies in the programmability and molecular recognition versatility of nucleic acids. Key methodologies include: (1) aptamers for specific protein recognition, often integrated with engineered DNA nanostructures (tetrahedrons, origami) to enhance binding avidity and spatial control; (2) enzyme-free catalytic amplification strategies (hybridization chain reaction – HCR, catalytic hairpin assembly – CHA, DNAzymes) enabling localized signal enhancement critical for low-abundance targets; (3) synergistic coupling of isothermal nucleic acid amplification techniques (rolling circle amplification – RCA, loop-mediated isothermal amplification – LAMP) with CRISPR-Cas systems (*e.g.*, Cas13a, Cas12a) for ultra-specific, amplified

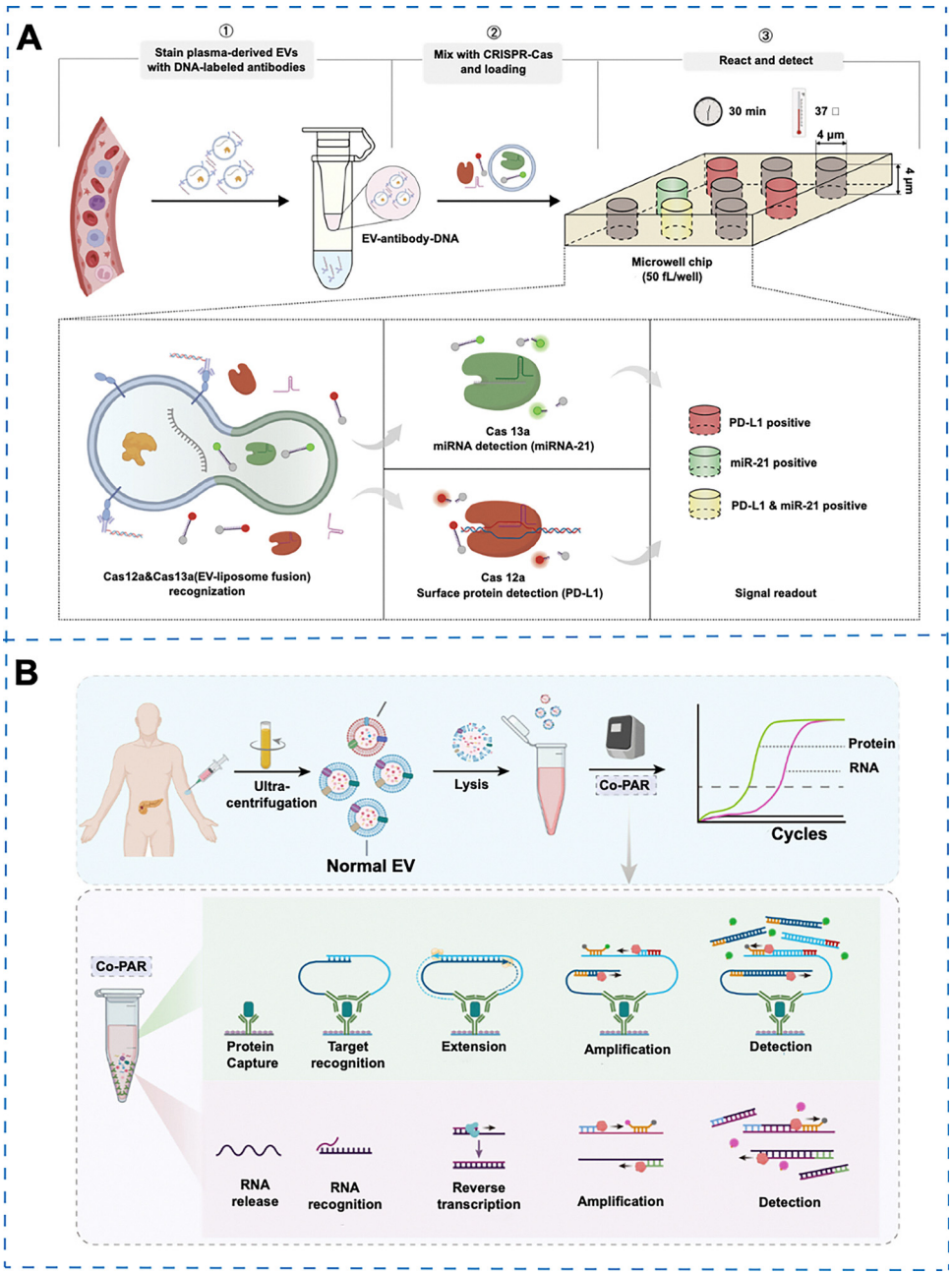

Fig. 8 Simultaneous detection of proteins and nucleic acids in EVs. (A) Concurrent detection of protein and miRNA at the sEVs level using a digital dual CRISPR-Cas assay. Reproduced with permission.[184] Copyright: 2025, American Chemical Society. (B) Codetection of proteins and RNAs onEVs for pancreatic cancer early diagnosis. Reproduced with permission.[187] Copyright: 2024, American Chemical Society.

detection of EV RNA cargoes, particularly microRNAs; and (4) DNA barcoding frameworks facilitating highly multiplexed biomarker profiling. These approaches collectively enable comprehensive molecular characterization of EVs at unprecedented resolution.

However, the translation of DNA-based EV detection into robust clinical tools faces several interconnected challenges. The development of high-affinity, high-specificity aptamers against complex EV membrane proteins remains a significant bottleneck, often requiring lengthy selection processes (SELEX) and sometimes yielding ligands with suboptimal affinity compared to monoclonal antibodies. While EV heterogeneity (in size, cargo, and origin) presents a specific challenge for reliable subpopulation detection, it is compounded by broader technical hurdles. The complex matrix of clinical biofluids (serum, plasma) introduces substantial interference through non-specific binding (biofouling) and background noise, demanding advanced sample preparation and anti-fouling strategies. Furthermore, the field lacks standardized protocols, universally accepted reference materials, and rigorous cross-platform validation frameworks, hindering reproducibility and clinical adoption. Practical implementation of highly multiplexed DNA barcoding at the single-EV level also faces

scalability issues related to probe diversity, efficient multi-target binding, cost-effective high-sensitivity readouts, and complex data management.

Future advancements in DNA-based EV detection hinge on strategic innovations across multiple fronts. Computational approaches leveraging artificial intelligence (AI) and structural modeling hold promise for *in silico* design and optimization of high-performance aptamers, nanostructures, and functional probes (*e.g.*, aptamer beacons), accelerating development cycles. To address EV heterogeneity, the development of single-EV analysis technologies is crucial. Techniques such as high-resolution flow cytometry, single-EV mass spectrometry (*e.g.*, CyTOF), and super-resolution microscopy are Essential for deconstructing heterogeneous populations and identifying definitive surface markers that can distinguish EV subclasses (*e.g.*, exosomes *vs.* microvesicles *vs.* apoptotic bodies) with greater certainty. Engineering next-generation DNA nanomaterials with enhanced *in situ* stability, nuclease resistance, biocompatibility, and signal efficiency including robust nanostructures, dynamic probes, and functional materials like DNA hydrogels, is crucial for improved performance in complex environments. Integration with microfluidic platforms is essential for creating automated, sample-to-answer systems capable of integrated EV isolation, processing, target extraction, DNA probe interaction, amplification, and multiplexed detection, enhancing throughput and enabling point-of-care applications. Importantly, rigorous clinical validation in large-scale, multi-center prospective cohorts is indispensable to demonstrate the diagnostic, prognostic, and predictive utility of DNA-based EV detection panels for specific diseases (*e.g.*, early-stage cancer, neurological disorders), establishing their clinical relevance and value.

In summary, DNA detection technology provides a versatile and powerful foundation for EV analysis, driving capabilities in sensitivity, specificity, multiplexing, and single-particle resolution. Overcoming persistent challenges in aptamer generation, matrix interference, standardization, and scalable multiplexing requires concerted interdisciplinary efforts. Success in computational design, advanced materials engineering, microfluidic integration, and comprehensive clinical validation will be paramount. These advancements will solidify DNA-based approaches as transformative tools in precision diagnostics and liquid biopsy, enabling the reliable detection and characterization of clinically relevant EV signatures. The inherent heterogeneity of EVs underscores the necessity of these sophisticated DNA-driven capabilities but remains one facet of the broader technical and translational landscape that these technologies are uniquely positioned to address.

Conflicts of interest

The authors declare that there is no conflict of interest.

Data availability

No primary research results, software or code have been included and no new data were generated or analysed as part of this review.

References

1 P. Wolf, *Br. J. Haematol.*, 1967, **13**, 269–288.
2 L. Doyle and M. Wang, *Cells*, 2019, **8**(7), 727.
3 R. Kalluri and V. S. LeBleu, *Science*, 2020, **367**(6478), aau6977.
4 J. M. Gudbergsson, K. Jonsson, J. B. Simonsen and K. B. Johnsen, *J. Controlled Release*, 2019, **306**, 108–120.
5 D. M. Pegtel and S. J. Gould, *Annu. Rev. Biochem.*, 2019, **88**, 487–514.
6 W. Yu, J. Hurley, D. Roberts, S. K. Chakrabortty, D. Enderle, M. Noerholm, X. O. Breakefield and J. K. Skog, *Ann. Oncol.*, 2021, **32**(4), 466–477.
7 K. O'Brien, K. Breyne, S. Ughetto, L. C. Laurent and X. O. Breakefield, *Nat. Rev. Mol. Cell Biol.*, 2020, **21**(10), 585–606.
8 M. A. Mori, R. G. Ludwig, R. Garcia-Martin, B. B. Brandao and C. R. Kahn, *Cell Metab*, 2019, **30**(4), 656–673.
9 G. van Niel, D. R. F. Carter, A. Clayton, D. W. Lambert, G. Raposo and P. Vader, *Nat. Rev. Mol. Cell Biol.*, 2022, **23**(5), 369–382.
10 M. Tkach and C. Thery, *Cell*, 2016, **164**(6), 1226–1232.
11 G. van Niel, G. D'Angelo and G. Raposo, *Nat. Rev. Mol. Cell Biol.*, 2018, **19**(4), 213–228.
12 R. Kalluri and K. M. McAndrews, *et al.*, *Cell*, 2023, **186**(8), 1610–1626.
13 M. Mathieu, L. Martin-Jaular, G. Lavieu and C. Théry, *Nat. Cell Biol*, 2019, **21**(1), 9–17.
14 Z. Yu and L. Pan, *et al.*, *Biosens. Bioelectron.*, 2023, **237**, 115526.
15 Y. Chen and X. Ma, *et al.*, *Sens. Actuators, B*, 2024, **399**, 134813.
16 C. Yuan and F. Zhou, *et al.*, *ChemBioChem*, 2024, e202400227.
17 K. W. Witwer and C. Théry, *J. Extracell. Vesicles*, 2019, **8**, 1648167.
18 A. S. Abdel Halim, H. A. Rudayni, A. A. Chaudhary and M. A. Ali, *J. Cell. Physiol.*, 2023, **238**, 32–69.
19 A. P. Ramos, H. G. Sebinelli, P. Ciancaglini, N. Rosato, S. Mebarek, R. Buchet, J. L. Millán and M. Bottini, *J. Extracell. Biol.*, 2022, **1**, e34.
20 M. Mathieu, N. Nevo, M. Jouve, J. I. Valenzuela, M. Maurin, F. J. Verweij, R. Palmulli, D. Lankar, F. Dingli and D. Loew, *et al.*, *Nat. Commun.*, 2021, **12**(1), 4389.
21 S. H. Hilton and I. M. White, *Sens. Actuators Rep.*, 2021, **3**, 100052.
22 J. Jankovicova, P. Secova, K. Michalkova and J. Antalikova, *Int. J. Mol. Sci.*, 2020, **21**(20), 7568.
23 Z. Andreu and M. Yanez-Mo, *Front. Immunol.*, 2014, **5**, 442.
24 T. Juan and M. Furthauer, *Cell Dev. Biol.*, 2018, **74**, 66–77.
25 T. Matsui, F. Osaki, S. Hiragi, Y. Sakamaki and M. Fukuda, *EMBO Rep*, 2021, **22**(5), e51475.
26 C. Caruso Bavisotto, A. Marino Gammazza, C. Campanella, F. Bucchieri and F. S. Cappello, *Cancer Biol*, 2022, **86**(Pt 1), 36–45.
27 Z. Albakova, M. K. S. Siam, P. K. Sacitharan, R. H. Ziganshin, D. Y. Ryazantsev and A. M. Sapozhnikov, *Transl. Oncol.*, 2021, **14**(2), 100995.

28 B. Van den Broek, C. Wuyts and J. Irobi, *J. Adv. Drug Delivery Rev.*, 2021, **179**, 114009.
29 M. A. Rogers, F. Buffolo, F. Schlotter, S. K. Atkins, L. H. Lee, A. Halu, M. C. Blaser, E. Tsolaki, H. Higashi and K. Luther, *et al.*, *Sci. Adv.*, 2020, **6**(38), eabb1244.
30 L. Zhang, P. Yang, J. Chen, Z. Chen, Z. Liu, G. Feng, F. Sha, Z. Li, Z. Xu and Y. Huang, *Nat. Commun.*, 2023, **14**, 5524.
31 M. Fu, Q. Gao, M. Xiao, R. F. Li, X. Y. Sun, S. L. Li, X. Peng and X. Y. Ge, *Cancer Res*, 2024, **84**, 2484–2500.
32 L. Xing, Z. Wang, Y. Feng, H. Luo, G. Dai, L. Sang, C. Zhang and J. Qian, *Cancer Immunol. Immunother.*, 2024, **73**, 145.
33 Y. Dai, Y. Wang, Y. Cao, P. Yu, L. Zhang, Z. Liu, Y. Ping, D. Wang, G. Zhang and Y. Sang, *et al.*, *Front. Oncol.*, 2021, **11**, 777684.
34 H. Sharma, V. Yadav, A. Burchett, T. Shi, S. Senapati, M. Datta and H. C. Chang, *Biosens. Bioelectron.*, 2025, **267**, 116848.
35 H. Li and C. Chiang, *et al.*, *Adv. Sci.*, 2024, **11**, e2306373.
36 M. H. Jeong and T. Son, *et al.*, *Adv. Sci.*, 2023, **10**, e2205148.
37 B. V. Sinn and G. von Minckwitz, *et al.*, *Ann. Oncol.*, 2013, **24**, 2316–2324.
38 S. S. Pinho, I. Alves and J. Gaifem, *et al.*, *Cell. Mol. Immunol.*, 2023, **20**, 1101–1113.
39 J. Macedo-da-Silva, V. F. Santiago and L. Rosa-Fernandes, *et al.*, *Mol. Immunol.*, 2021, **135**, 226–246.
40 M. Yang, Y. Zhang, M. Li, X. Liu and M. Darvishi, *Cancer Cell Int.*, 2023, **23**, 24.
41 Y. Wei, Z. Wang, Z. Qin, Q. Wan, Y. Li, F. R. Tay, C. Wang, T. Zhang and L. Niu, *BMEMat*, 2024, **3**, e12127.
42 J. Yu and R. Zhou, *et al.*, *Anal. Chem.*, 2025, **97**, 5355–5371.
43 A. S. Doghish and M. S. Elballal, *et al.*, *Pathol., Res. Pract.*, 2023, **243**, 154375.
44 L. Zhang, T. Wu and Y. Shan, *et al.*, *Brain*, 2021, **144**, 3421–3435.
45 M. Wang, F. Yu, P. Li and K. Wang, *Mol. Ther. Nucleic Acids*, 2020, **21**, 367–383.
46 X. Pu, C. Zhang and G. Ding, *et al.*, *Transl. Oncol.*, 2024, **40**, 101847.
47 L. T. Nguyen, J. Zhang and X. Y. Rima, *et al.*, *J. Extracell. Vesicles*, 2022, **11**, e12258.
48 M. Hu, V. Brown and J. M. Jackson, *et al.*, *Anal. Chem.*, 2023, **95**, 7665–7675.
49 P. S. Suresh, S. Thankachan and T. Venkatesh, *et al.*, *Mol. Biotechnol.*, 2023, **65**, 300–310.
50 G. Lu, X. Jiang and A. Wu, *et al.*, *Front. Microbiol.*, 2021, **12**, 642559.
51 C. D. M. Campos, K. Childers and S. S. T. Gamage, *Annu. Rev. Anal Chem. (Palo Alto Calif)*, 2021, **14**, 207–229.
52 R. T. Miceli, T. Y. Chen and Y. Nose, *et al.*, *J. Extracell. Vesicles*, 2024, **13**, e70005.
53 H. Wijerathne, M. A. Witek and J. M. Jackson, *et al.*, *Commun. Biol.*, 2020, **3**, 613.
54 Z. Zhao, H. Wijerathne and A. K. Godwin, *et al.*, *Nucl. Acids*, 2021, **2**, 80.
55 J. Elzanowska, C. Semira and B. Costa-Silva, *Mol. Oncol.*, 2021, **15**, 1701–1714.
56 J. Ghanam, V. K. Chetty and L. Barthel, *et al.*, *Cell Biosci*, 2022, **12**, 37.
57 B. J. Sanders, D. C. Kim and R. C. Dunn, *Anal. Methods*, 2016, **8**(39), 7002–7013.
58 S. Khodashenas, S. Khalili and M. F. Moghadam, *Biotechnol. Lett.*, 2019, **41**, 523–531.
59 V. Pospichalova, J. Svoboda, Z. Dave and A. Kotrbova, *et al.*, *J. Extracell. Vesicles*, 2015, **4**, 25530.
60 H. Wang, H. Peng, J. Wang, Z. Qin and L. Xue, *Clin. Epigenet.*, 2018, **10**, 59.
61 Y. X. Chen, K. J. Huang and K. X. Niu, *Biosens. Bioelectron.*, 2018, **99**, 612–624.
62 C. Tuerk and L. Gold, *Science*, 1990, **249**, 505–510.
63 A. D. Ellington and J. W. Szostak, *Nature*, 1990, **346**, 818–822.
64 S. Xiao and Y. Yao, *et al.*, *Nano Lett*, 2023, **23**, 8115–8125.
65 C. V. Pham, *et al.*, *J Extracell Vesicles*, 2024, **13**, e12502.
66 J. Li and Y. Li, *et al.*, *Angew. Chem., Int. Ed.*, 2023, **63**(Issue 4), e202314262.
67 Y. Wang and Y. Jie, *et al.*, *Anal. Chem.*, 2023, **95**, 18166–18173.
68 X. Yu, Y. Cao and J. Xia, *et al.*, *Anal. Chem.*, 2025, **97**, 11073–11081.
69 K. Chang and Y. Fang, *et al.*, *Anal. Chem.*, 2023, **95**, 16194–16200.
70 Q. Wu and Q. Wu, *et al.*, *Anal. Chem.*, 2025, **97**, 5313–5323.
71 C. Liu, J. Zhao and F. Tian, *et al.*, *J. Am. Chem. Soc.*, 2019, **141**, 3817–3821.
72 Y. Zhang and Q. Wu, *Anal. Chem.*, 2023, **95**, 9373–9379.
73 X. Yao and Y. Wang, *et al.*, *Anal Chem.*, 2025, **97**, 15225–15233.
74 Y. Ren, K. Ge, Q. Tang and X. Liang, *et al.*, *Anal. Chem.*, 2024, **96**, 9585–9592.
75 J. Zhou and Q. Lin, *et al.*, *Anal. Chem.*, 2022, **94**, 5723–5728.
76 X. Meng, X. Zhou, W. Yan and D. Chen, *et al.*, *Nano Lett*, 2025, **25**, 10354–10361.
77 X. Chen, Y. Deng, R. Niu, Z. Sun and A. Batool, *et al.*, *Anal. Chem.*, 2022, **94**, 13019–13027.
78 Y. Zhang and D. Wang, *et al.*, *ACS Sens.*, 2019, **4**, 3210–3218.
79 X. Meng and X. Pang, *et al.*, *Anal. Chem.*, 2024, **96**, 13299–13307.
80 X. Liu, J. Zhang, Z. Chen and X. He, *et al.*, *Biosens. Bioelectron.*, 2025, **267**, 116737.
81 W. Shen, K. Guo and G. B. Adkins, *et al.*, *Angew. Chem., Int. Ed.*, 2018, **57**, 15675–15680.
82 C. Fan, N. Zhao, K. Cui and G. Chen, *et al.*, *ACS Sens*, 2021, **6**, 3234–3241.
83 X. Li and Y. Liu, *et al.*, *ACS Nano*, 2024, **18**, 11389–11403.
84 Y. Feng, Y. Yang, Y. Xiao and T. Fu, *et al.*, *Anal. Chem.*, 2023, **95**, 1132–1139.
85 S. Yang, L. Zhou, Z. Fang and Y. Wang, *et al.*, *ACS Sens.*, 2024, **9**, 2194–2202.
86 B. Bo, W. Li, J. Li and C. Han, *et al.*, *ACS Appl. Mater. Interfaces*, 2023, **15**, 17696–17704.
87 W. Tan, C. Zhang and S. Cheng, *et al.*, *Anal. Chem.*, 2024, **96**, 1328–1335.

88 X. Yao, H. Shi, S. Wu and X. Xue, *et al.*, *Anal. Chem.*, 2025, **97**, 14369–14376.
89 X. Zhao, L. Zeng, Q. Mei and Y. Luo, *et al.*, *ACS Sens.*, 2020, **5**, 2239–2246.
90 L. Yang, J. Zhang and J. Zhang, *et al.*, *Anal. Chem.*, 2025, **97**, 2176–2185.
91 R. Huang and L. Song, *et al.*, *Nanoscale*, 2020, **12**, 2445–2451.
92 B. Lin and T. Tian, *et al.*, *Angew. Chem., Int. Ed.*, 2021, **60**, 7582–7586.
93 M. Ye, L. Mou, J. Feng, L. Wu and D. Jin, *et al.*, *Anal. Chem.*, 2025, **97**, 2343–2350.
94 J. Wu, Z. Lin, Z. Zou and S. Liang, *et al.*, *J. Am. Chem. Soc.*, 2022, **144**, 23483–23491.
95 Y. Huang and F. Zhou, *et al.*, *Electrochem. Commun.*, 2023, **156**, 107580.
96 X.-W. Zhang, G.-X. Qi and S. Chen, *et al.*, *Anal. Chem.*, 2024, **96**, 10800–10808.
97 X. Gao and X. Teng, *ACS Sens.*, 2021, **6**, 3611–3620.
98 H. Xu and Y. Zhang, *Anal. Chem.*, 2025, **97**, 15282–15289.
99 J. Zhang, J. Shi and H. Zhang, *et al.*, *J Extracell Vesicles*, 2020, **10**, e12025.
100 J. Ma, K. Li, Z. Duan and X. Yang, *et al.*, *Anal. Chem.*, 2025, **97**(13), 7483–7489.
101 Y. Sun and Y. Wang, *et al.*, *Chem*, 2021, **93**, 12383–12390.
102 Q. Mei, B. Gu, Y. Jiang and Y. Wang, *et al.*, *ACS Omega*, 2024, **9**(13), 15350–15356.
103 Y. Yu, Q. Guo and W. Jiang, *et al.*, *Anal. Chem.*, 2021, **93**, 11298–11304.
104 R. Huang, L. He, Y. Xia and H. Xu, *et al.*, *Small*, 2019, **15**, 1900735.
105 G. Zhang, Y. Wang, W. Zhou and Y. Lei, *et al.*, *Angew. Chem., Int. Ed.*, 2023, **62**, e202315113.
106 Y. Li and J. Wang, *Anal. Chem.*, 2021, **93**, 9860–9868.
107 R. Martel, M. L. Shen and P. DeCorwin-Martin, *et al.*, *ACS Sens.*, 2022, **7**, 3817–3828.
108 F. Xu, K. Wang, C. Xu and J. Xu, *et al.*, *Anal. Chem.*, 2025, **97**, 9212–9219.
109 Y. Ren, K. Ge, W. Lu, X. Xie and Y. Lu, *et al.*, *ACS Appl. Mater. Interfaces*, 2023, **15**, 55358–55368.
110 Z. Lu and Y. Shi, *et al.*, *Anal. Chem.*, 2022, **94**, 9466–9471.
111 S. Saroj, D. Paul, A. Ali and C. Andreou, *et al.*, *ACS Appl. Bio Mater*, 2023, **6**, 4944–4951.
112 S. Nath and P. Mukherjee, *Trends Mol. Med.*, 2014, **20**, 332–342.
113 W. Chen, Z. Zhang and S. Zhang, *et al.*, *Int. J. Mol. Sci.*, 2021, **22**, 6567.
114 X. Mao, S. K. Tey and C. L. S. Yeung, *et al.*, *Adv. Sci.*, 2020, **7**, 2002157.
115 T. Sakaue, H. Koga, H. Iwamoto and T. Nakamura, *et al.*, *Med. Mol. Morphol.*, 2019, **52**(4), 198–208.
116 L. Zhu and Y. Xu, *et al.*, *Angew. Chem., Int. Ed.*, 2021, **60**, 18111–18115.
117 K. Luo, Z. Jiang, L. Li and L. Lin, *et al.*, *ACS Sens.*, 2025, **10**(8), 5528–5538.
118 P. Li, Q. Chang, M. Liu, K. Lei and S. Ping, *et al.*, *Anal. Chem.*, 2023, **95**, 17467–17476.
119 H. Wang and J. Zeng, *Angew. Chem., Int. Ed.*, 2022, **61**, e202116932.
120 R.-Y. Zhang, S.-H. Luo and X.-M. Lin, *et al.*, *Anal. Chim. Acta*, 2021, **1157**, 338396.
121 H. Zhu, S. Chen and F. Lan, *et al.*, *Anal. Chim. Acta*, 2024, **1311**, 342704.
122 H. Zhu and S. Chen, *et al.*, *J. Nanobiotechnol.*, 2023, **21**, 328.
123 W. Li, W. Wang and S. Luo, *Anal. Chem.*, 2024, **96**, 4909–4917.
124 J. Peng, B. Li, Z. Ma and Z. Qiu, *et al.*, *Talanta*, 2025, **281**, 126838.
125 P. Miao and Y. Tang, *et al.*, *Anal. Chem.*, 2020, **92**, 12026–12032.
126 R. Wang and X. Zhao, *et al.*, *Anal. Chem.*, 2020, **92**, 2176–2185.
127 H. Yan, Y. Wen, Z. Tian and N. Hart, *et al.*, *Nat. Biomed. Eng*, 2023, **7**, 1583–1601.
128 Z. Zhang, X. Liu, C. Peng and R. Du, *et al.*, *ACS Nano*, 2025, **19**, 10013–10025.
129 Z. Xie, S. Zhao, R. Deng and X. Tang, *et al.*, *ACS Nano*, 2025, **19**, 12222–12236.
130 L. Luo, F. Dong, D. Li, X. Li and X. Li, *et al.*, *ACS Sens*, 2024, **9**, 1438–1446.
131 J. Song, M. H. Cho and H. Cho, *et al.*, *Nat Biotechnol*, 2024, DOI: **10.1038/s41587-024-02426-6**.
132 S. Zhand, Y. Zhu and H. Nazari, *et al.*, *Anal. Chem.*, 2023, **95**(6), 3228–3237.
133 X. Zhang, X. Wei, J. Qi, J. Shen and J. Xu, *et al.*, *Anal. Chem.*, 2022, **94**, 4787–4793.
134 S. Zhu and J. Chen, *et al.*, *Scient. Rep.*, 2024, **14**, 11217.
135 M. Zhou, C. Li, R. Wei and H. Wang, *et al.*, *Anal. Chem.*, 2024, **96**, 4322–4329.
136 J. Qian, Q. Zhang and M. Liu, *et al.*, *Biosens. Bioelectron.*, 2022, **196**, 113707.
137 D. Sulaiman and N. Juthani, *Adv. Healthcare Mater.*, 2022, **11**, 2102332.
138 D. Yu, J. Gu, J. Zhang and M. Wang, *et al.*, *ACS Nano*, 2025, **19**, 10078.
139 N. Sun, B. V. Tran and Z. Peng, *et al.*, *Adv. Sci.*, 2022, **9**, 2105853.
140 L. Yang and H. Guo, *et al.*, *Anal. Chem.*, 2023, **95**, 17834–17842.
141 P. Liu, X. Qian, X. Li and L. Fan, *et al.*, *ACS Appl. Mater. Interfaces*, 2020, **12**, 45648–45656.
142 B. Shen, L. Li and C. Liu, *et al.*, *Anal. Chem.*, 2023, **95**, 4486–4495.
143 L. Zou, Z. Wu, X. Liu and Y. Zheng, *et al.*, *Anal. Chem.*, 2020, **92**, 11953–11959.
144 L. Shi, H. Cai and H. Wang, *et al.*, *Anal. Chem.*, 2023, **95**, 17662–17669.
145 W. Cheng, H. Pan and J. Chen, *et al.*, *Anal. Chem.*, 2025, **97**, 5244–5250.
146 N. Liu, H. Lu, L. Liu, W. Ni and Q. Yao, *et al.*, *Anal. Chem.*, 2021, **93**, 5917–5923.
147 M. Chen, S. Lin, C. Zhou, D. Cui, H. Haick and N. Tang, *Adv. Healthc. Mater.*, 2023, **12**(8), 2202437.

148 A. M. Silva, E. Lázaro-Ibáñez and A. Gunnarsson, *et al.*, *J. Extracell. Vesicles*, 2021, **10**(10), e12130.
149 M. Xie, F. Wang and J. Yang, *et al.*, *Anal. Chem.*, 2022, **94**, 13043–13051.
150 J. Feng, Y. Shu, Y. An and Q. Niu, *et al.*, *Anal. Chem.*, 2023, **95**, 7743–7752.
151 X. Gao and F. Ding, *et al.*, *Angew. Chem., Int. Ed.*, 2019, **58**, 8719–8723.
152 E. M. Clarissa, S. Kumar and J. Park, *et al.*, *ACS Nano*, 2025, **19**, 5526–5538.
153 L. Cui, R. Peng and C. Zeng, *et al.*, *Nano Today*, 2022, **46**, 101599.
154 C. Park, S. Chung, H. Kim and N. Kim, *et al.*, *ACS Nano*, 2024, **18**, 26297–26314.
155 L. Meng, L. Wang and Z. Sun, *et al.*, *Adv. Healthcare Mater.*, 2025, **14**, 2404981.
156 J. Zhang, M. Guan and C. Ma, *et al.*, *ACS Sens*, 2023, **8**, 565–575.
157 M. Xiao, X. Wang and Q. Yao, *et al.*, *Chem*, 2024, **10**, 3634–3643.
158 Y. Cao, X. Yu and T. Zeng, *et al.*, *J. Am. Chem. Soc.*, 2022, **144**, 13475–13486.
159 J. Hong and T. Song, *Adv. Sci.*, 2023, **10**, 2301766.
160 B. Ning, Z. Huang and B. M. Youngquist, *et al.*, *Nat. Nanotechnol.*, 2021, **16**(9), 1039–1044.
161 J. H. Lee, J. A. Kim and M. H. Kwon, *et al.*, *Biomaterials*, 2015, **54**, 116e125.
162 C. Qian, Y. Xiao and J. Wang, *et al.*, *Sens. Actuators, B*, 2021, **333**, 129559.
163 F. Zhou and L. Pan, *et al.*, *Anal. Chem.*, 2024, **96**, 15665–15673.
164 D. Mao, M. Zheng, W. Li and Y. Xu, *et al.*, *Biosens Bioelectron*, 2022, **204**, 114077.
165 J. Chen and M. Xie, *et al.*, *Anal. Chem.*, 2022, **94**, 2227–2235.
166 W. Liu, H. Yang, X. Liu and H. Cai, *et al.*, *Anal. Chem.*, 2025, **97**, 4233–4240.
167 S. Zhao, S. Zhang, H. Hu and Y. Cheng, *et al.*, *Angew. Chem., Int. Ed.*, 2023, **62**, e202303121.
168 S. Jiang, Q. Li, C. Wang and Y. Pang, *et al.*, *ACS Sens*, 2021, **6**, 852–862.
169 B. Liu, D. Zhao, J. Chen and M. Shi, *et al.*, *Anal. Chem.*, 2024, **96**, 1733–1741.
170 J. Zhao, C. Liu, Y. Li and Y. Ma, *et al.*, *J. Am. Chem. Soc.*, 2020, **142**, 4996–5001.
171 X.-W. Zhang, G.-X. Qi and M.-X. Liu, *et al.*, *ACS Sens*, 2024, **9**, 1555–1564.
172 S. Sharma, X. Jiao, J. Yang and K. Y. Kwan, *et al.*, *Nat. Cell Biol*, 2025, **27**, 983–991.
173 T. Ren, Y. Zhang, Y. Tong and Q. Zhang, *et al.*, *Nat. Commun*, 2025, **16**, 3391.
174 X. Wang, L. Tian, J. Lu and I. O. Ng, *Oncogenesis*, 2022, **11**, 54.
175 Y. Liang, B. M. Lehrich, S. Zheng and M. Lu, *J. Extracell. Vesicles*, 2021, **10**(7), e12090.
176 A. Valentino, P. Reclusa and R. Sirera, *et al.*, *Clin. Transl. Oncol.*, 2017, **19**(6), 651–657.
177 X. Yu, M. Odenthal and J. W. Fries, *Int. J. Mol. Sci.*, 2016, **17**(12), 2028.
178 J. Wu and Z. Shen, *Cancer Med.*, 2020, **9**(19), 6909–6922.
179 C. C. Hsu, Y. Yang, E. Kannisto, X. Zeng and G. Yu, *et al.*, *ACS Nano*, 2023, **17**(9), 8108–8122.
180 S. Rossetti and N. Sacchi, *Cancers (Basel)*, 2019, **11**(2), 130.
181 B. Madhavan, S. Yue, U. Galli, S. Rana and W. Gross, *et al.*, *Int. J. Cancer*, 2015, **136**(11), 2616–2627.
182 J. Lee, S. Lee, H. Lee and T. T. P. Tran, *et al.*, *ACS Biomater. Sci. Eng.*, 2023, **9**, 6369–6378.
183 S. Zhou, T. Hu and G. Han, *et al.*, *Small*, 2020, **16**, 2004492.
184 X. Xu, Y. Zhang, J. Liu and S. Wei, *et al.*, *ACS Nano*, 2025, **19**, 1271–1285.
185 Z. Troyer, O. Gololobova and A. Koppula, *et al.*, *ACS Nano*, 2024, **18**, 26568–26584.
186 K. T. Nguyen, X. Y. Rima and L. T. H. Nguyen, *et al.*, *Adv. Healthcare Mater.*, 2025, **14**, 2400622.
187 J. He, J. Long, C. Zhai and J. Xu, *et al.*, *Anal. Chem.*, 2024, **96**, 6618–6627.
188 X. Qin, Y. Xiang, N. Li and B. Wei, *et al.*, *Biosens Bioelectron*, 2022, **216**, 114636.
189 Z. Dong, C. Tang and Z. Zhang, *et al.*, *ACS Appl. Bio Mater.*, 2020, **3**, 2560–2567.